Interscience Research Network

Interscience Research Network

Conference Proceedings - Full Volumes | IRNet Conference Proceedings

3-4-2012

Proceedings of International Conference on Power System Operation and Energy Management

Prof.Srikanta Patnaik Mentor
IRNet India, patnaik_srikanta@yahoo.co.in

Follow this and additional works at: https://www.interscience.in/conf_proc_volumes

 Part of the Biomedical Commons, Controls and Control Theory Commons, Electrical and Electronics Commons, Electromagnetics and Photonics Commons, Electronic Devices and Semiconductor Manufacturing Commons, Nanotechnology Fabrication Commons, Power and Energy Commons, Signal Processing Commons, Systems and Communications Commons, and the VLSI and Circuits, Embedded and Hardware Systems Commons

Recommended Citation

Patnaik, Prof.Srikanta Mentor, "Proceedings of International Conference on Power System Operation and Energy Management" (2012). *Conference Proceedings - Full Volumes*. 62.
https://www.interscience.in/conf_proc_volumes/62

This Book is brought to you for free and open access by the IRNet Conference Proceedings at Interscience Research Network. It has been accepted for inclusion in Conference Proceedings - Full Volumes by an authorized administrator of Interscience Research Network. For more information, please contact sritampatnaik@gmail.com.

Proceedings

of

International Conference

on

POWER SYSTEM OPERATION AND ENERGY MANAGEMENT

(ICPSOEM)

March 4th, 2012

Editor-in-Chief

Prof. (Dr.) Srikanta Patnaik
President, IRNet India
Intersceince Campus, Bhubaneswar
Mailto: iccsit.guwahati@gmail.com

Organized by:

About **ICPSOEM 2012**

In spite of so many advancements in the power and energy sector over the last two decades, its survival to cater quality power with due consideration for planning, coordination, marketing, safety, stability, optimality and reliability is still believed to remain critical. Though it appears simple from the outside, yet the internal structure of large scale power systems is so complex that event management and decision making requires a formidable preliminary preparation, which gets still worsened in the presence of uncertainties and contingencies. These aspects have attracted several researchers to carryout continued research in this field and their valued contributions have been significantly helping the newcomers in understanding the evolutionary growth in this sector, starting from phenomena, tools, methodologies to strategies so as to ensure smooth, stable, safe, reliable and economic operation. This journal shall provide a new forum for dissemination of knowledge on both theoretical and applied research spreading over various fundamental and application fields of electric power systems with an ultimate aim to bridge the gap between these coherent disciplines of knowledge. This forum would accelerate interaction between the above bodies of knowledge with an aim to foster unified development in the next generation.

This conference aims at bringing researchers, electrical engineers and professionals who are working in this area to deliberate on this topic. Papers will be reviewed by at least two referees each.

Suitable research topics include but are not limited to:

The conference invites papers from all areas under the broad spectrum of power system planning, coordination, marketing, safety, stability, security, optimality, economy, reliability and their applications. The areas are as follows:

- Power system modeling, simulation and analysis
- Power system stability, dynamics and control
- Power generation, transmission and distribution
- Flexible AC Transmission
- High voltage engineering and insulation coordination
- Distributed generation systems, micro grid operation and wind power systems
- Power Quality and demand side management
- Power system protection and digital relaying
- Energy management policy planning and decision making
- Network restructuring and marketing strategy
- Power system optimization
- Economic load dispatch

- State estimation and security analysis
- Reliability analysis
- Modeling uncertainties and contingencies
- Fault detection and diagnosis
- Deregulation of electricity market
- Distribution automation
- Machines, power electronics and drives
- Computer applications in power systems
- Soft computing applications in power systems
- Power system communication
- Renewable energy management
- Hybrid energy systems
- Power system instrumentation
- Energy conservation and management
- Fuel cells and batteries
- Nuclear power alternatives
- Remote sensing, telemetry, and signal processing
- Application of nano-technology
- Recent trends and issues
- Use of super conductors in power systems
- Energy efficient protocols, tools and gadgets
- Microprocessor based applications
- Supervisory control and data acquisition

ORGANIZING COMMITTEE

Chief Patron/ Program Chair:

Prof. (Dr.) Srikanta Patnaik
President IRNet & Chairman, I.I.M.T., Bhubaneswar
Intersceince Campus,
At/Po.: Kantabada, Via-Janla, Dist-Khurda
Bhubaneswar, Pin:752024. Orissa, INDIA

Secretary IRNet:

Prof. Pradeep Kumar Mallick
IIMT, Bhubaneswar
Email:pradeepmallick84@gmail.com
Mobile No: 08895885152

Conference Coordinator:

Event Manager
Prof. Sharada Prasad Sahoo.
IIMt, Bhubaneswar

Publication

Prof. Sushanta Kumar Panigrahi
Prof. Mritunjay Sharma
IIMT, Bhubaneswar

Post Conference Coordinator

Bibhu Prasad Mohanty
Mob:08895995279

Head (System & Utilities)
Prof. Sanjay Sharma
IIMT, Bhubaneswar

Members :

Rashmi Ranjan Nath
Ujjayinee Swain
Bikash Kumar Rout
Pritika Mohanty

.

First Impression : 2012

(c) Interscience Research Network

Proceedings of International Conference on

POWER SYSTEM OPERATION AND ENERGY MANAGEMENT

No part of this publication may be reproduced or transmitted in any form by any means, electronic or mechanical, including photocopy, recording, or any information storage and retrieval system, without permission in writing from the copyright owners.

DISCLAIMER

The authors are solely responsible for the contents of the papers complied in this volume. The publishers or editors do not take any responsibility for the same in any manner. Errors, if any, are purely unintentional and readers are requested to communicate such errors to the editors or publishers to avoid discrepancies in future.

ISBN : 978-93-81693-24-7

Published by :

IPM PVT. LTD., Interscience Campus
At/PO.: Kantabada, Via: Janla, Dist: Khurda, Pin- 752054
Publisher's Website : www.interscience.in
E-mail: ipm.bbsr@gmail.com

Typeset & Printed by :

IPM PVT. LTD.

TABLE OF CONTENTS

Sl. No.	Topic	Page No.
	Editorial - *Prof. (Dr.) Srikanta Patnaik*	
1	**Volt-Second Balance Method For Mitigation of Inrush Current in Single Phase Transformers** – *D P Balachandran, R Sreerama Kumar & B Jayanand*	01-06
2	**Design and Simulation of Modified Auxiliary Resonant Boost Converter for Solar Energy Based Systems** – *K. R. Sunil Raj & K. Manjunath*	07-12
3	**Investigation on Doubly Fed Induction Generator Steady State Parameters** – *Sunil Kumar, Nitin Goel & P.R. Sharma*	13-16
4	**Comparison of Varies Method for Energy Harvesting System from Piezoelectric Material** – *Milind S. Burle & Vyankateshwar.G. Girhepunje*	17-22
5	**Design of a Microcontroller Based PFC** – *Pradeep Kumar, P.R.Sharma & Ashok Kumar*	23-28
6	**Transient Analysis of EHVAC Circuit Breakers for Inductive and Capacitive Current Switching in 400kV IEEE 14bus System** – *Rajaramamohanarao Chennu, S Sudhakara Reddy, V S Nanda Kumar, M Chandra Sekahr & Maroti*	29-35
7	**Overview of Honeypot Security System for E-Banking** – *Prajakta Shirbhate, Vaishnavi Dhamankar, Aarti Kshirsagar, Purva Deshpande & Smita Kapse*	36-40
8	**Modeling of Green Energy Sources –A Solar and Wind Hybrid Model** – *Diksha Khare & SF.Lanjewar*	41-43
9	**Social Welfare Maximization in Deregulated Power System** – *Rekha Swami*	44-48
10	**The Factors Affecting Energy Management System Adoption for Smart Home : Marketing Survey Approach** – *Jyh-Yih Hsu & Jung-Jui Chang*	49-53

Editorial

The digitalization and mechanization of various power units across the world to manifest efficient production, storage, and distribution is gaining momentum in the sphere of academics and industrial research. The capitalistic advanced countries have exhibited investment behavior in the advanced digital and relay technologies, when it is a distant dream for progressing economies. The current research is to design optimization, control, and protection machinery for power systems. Although the discipline like electrical engineering has narrated academic maturity in the last decades, but the limitations of the non renewable energy sources, turbulence and disturbances in the energy propagation cascades various insightfulness and stimulation in post classical electrical era. Evidence shows that there are phenomenal supplements in power generation and control after the introduction of Energy Management System (EMS) supported by Supervisory Control and Data Acquisition (SCADA). As there is increasing focus on strengthening the capacity of the power houses with the existing resources or constraints some new dimensions like FACTS, Optimal System Generation, High Voltage DC transmission system, Power Generation Control, Soft Computing, Compensation of transmission line, Protection scheme of generator, Loss calculation, economics of generation, fault analysis in power systems are emerging. Since the world is suffering with water, food, and energy crisis,, energy consumption has social relevancy.

Keeping view of the ongoing energy and power issues many action research can be initiated by the research fraternity of this domain. The conference is a thought provoking outcome of all these interrelated facts. We take the privilege of organizing this conference for the first time in the city of Bhopal.

Prof. (Dr.) Srikanta Patnaik
President, IRNet India and Chairman IIMT
Intersceince Campus, Bhubaneswar
Email: patnaik_srikanta@yahoo.co.in

Volt-Second Balance Method For Mitigation of Inrush Current in Single Phase Transformers

D P Balachandran[1], R Sreerama Kumar[2] & B Jayanand[3]

[1]College of Engineering, Trivandrum, Kerala, India, [2]National Institute of Technology, Calicut Kerala, India
[3]Govt. Enginering College, Thrissur, Kerala, India

Abstract - During the transient period at the start of transformer energization, it experiences a flux linkage that is up to twice its nominal steady state value and saturates the core. This causes a large inrush current to flow which affects the power system stability and power quality especially when the source is weak. Sequential phase energization technique and addition of neutral resistor are the major methods for minimization of inrush current. This paper proposes a simple technique to limit the flux linkage during the time of transformer energization and prevents the flux saturation there by reducing the inrush current. This is based on a volt-second balance which injects a transient voltage to the primary of the transformer during inrush currents. The effectiveness of the proposed scheme is verified by simulation.

Keywords - *Inrush current, flux compensation, volt-second balance, voltage injection.*

I. INTRODUCTION

Transformer energization on no load results magnetizing inrush currents which is several times the nominal load current and last for a few cycles. The time taken by the inrush current to decay depends on the time constant of the transformer and the circuit parameters. Time constant of the transformer is not constant; the value of inductance changes depending on the extent of core saturation. During the first few cycles saturation is high and inductance is low. Hence the initial current and the rate of decay of current are high. As the resistance of the circuit damps and saturation drops, inductance increases slowing down the decay. Hence the decay of inrush current starts with a high initial rate and progressively reduces. The transient magnetizing inrush current of the switched-in transformer also flows into other transformers and produce in them a dc flux which gets superimposed on their normal ac flux [1].

The asymmetrical high magnitude inrush currents contain odd and even harmonics and a slowly decaying dc component. The high magnitude of inrush current may result in the advertent operation of the overload and differential relays, tripping the transformer out of the circuit as soon as it is switched on. The presence of harmonics may lead to resonance causing temporary over voltages. The other undesirable effects of inrush currents are oscillatory torque in motors, increased mechanical and insulation failure. The magnitude and

polarity of inrush current depends on several factors such as the reactive power demand in transformers causing voltage sag problems point on the voltage waveform at which transformer is energized, the residual flux building polarity and over excitation.

Several methods have been proposed for eliminating inrush current in transformers. Over sizing of transformer at more than rated flux density is one approach to avoid the inrush current. But this will increase the size and weight of the transformer. Re-energization of a transformer exactly at an instant of a voltage wave which corresponds to the actual flux density in the core at that instant, it would result in no inrush current [1]. Sequential energization of each phase with a grounding resistor connected at the transformer neutral reduces inrush current [2], [3], [4]. Elimination of inrush current is achieved by controlled transformer switching by taking into account the core flux and residual core flux in the closing control algorithm [5],[6]. However in practice the instant of switching cannot be easily controlled. In [7] the authors present a technique based on the use of a virtual air gap. A non-synchronous suppressing method is proposed in [8] to suppress the inrush current of phase transformers. Inrush currents in coupling transformers of voltage sag compensators are mitigated by controlling the injection voltage [9]. A thyristor controlled series compensator in transmission lines mitigates the impact of transformer inrush current by decreasing the source reactance [10].

In [11] a circuit breaker control strategy without independent pole operation and residual flux estimation has been reported for reducing inrush current. An active method of the series compensator used for reduction of

inrush current is explained in [12]. A method based on voltage injection to the tertiary winding of power transformers prior to primary side energization has been explained in [13]. This paper proposes a new method for minimizing the inrush current in transformers by injecting a compensatory current into the load transformer which compensates the additional flux built by the dc component of the inrush current and preventing saturation of core flux. The compensating current supplied by the series compensator has opposite polarity to the inrush current produced by the load transformer.

II. PHYSICAL PHENOMINA AND THEORY

When a transformer is re-energized by a voltage source, the flux linkage must match the voltage change according to Faraday's law,

$$V_m \sin(\omega t+\theta) = i_o R + N \frac{d\Phi m}{dt} \quad (1)$$

where ,

V_m - peak value of the applied voltage

θ - angle at which voltage is switched on

i_o - instantaneous value of magnetizing current

Φ_m - instantaneous value of flux

R - primary winding resistance

N - primary winding turns

The solution of the equation assuming linear magnetic characteristics (1) is,

$$\Phi_m = (\Phi_{mp}\cos\theta \pm \Phi_r)\ e^{-(\frac{R}{L})t} - (\Phi_{mp}\cos(\omega t+\theta)) \quad (2)$$

where, Φ_{mp} - peak flux

Φ_r - residual flux

The flux waveform given by equation (2) shows that the first component is a flux wave of transient dc component, which decays at a rate determined by the ratio of resistance to inductance of primary winding (R/L), and a steady-state ac component. This dc component drives the core strongly into saturation which is accompanied by flux unbalance and drop in inductance. The rate at which current in a coil increases is inversely proportional to the inductance and is given by

$$I = V*t/L^1 \quad (3)$$

where, I - rms value of current

V - rms value of voltage

t - time in seconds

L^1 - non linear inductance

Any drop in inductance therefore causes the current to raise faster, increasing the field strength and driving the core even further into saturation causing flux unbalance. The basic principle of the proposed inrush current minimization technique is to prevent the flux from exceeding the predetermined maximum flux (Φ_{mp}), and to keep the inductance of the transformer in steady state preventing the inrush current.

The expression for flux density in a transformer core is

$$B = (V \times t) / (N \times Ae) \quad (4)$$

where B - flux density in Tesla

Ae - cross sectional area of core in m^2

Examination of this expression reveals that core flux is a function of the applied volt-second and the physical characteristics of the magnetic design. Flux unbalance means volt-seconds unbalance. So flux balance is achieved by making volt-seconds balance by injecting a transient voltage to the transformer.

III. PROPOSED INRUSH CURRENT MITIGATION SCHEME

The simplified single line block diagram of the proposed inrush current mitigation technique is shown in Fig.1. The system consists of a pulse transformer connected in series with the primary winding of the load transformer for injecting the compensating flux (volt-second) into the load transformer. GTO1 and GTO2 are anti- parallel connected gate turn off switches connected across the pulse transformer. For an offline compensator system, the pulse transformer is bypassed by the GTO switches when the transformer grid current is normal. The inrush current detector detects the presence of inrush current and generates a mono pulse of short duration which opens GTO1 or GTO2 and closes thyristor T1/T2.

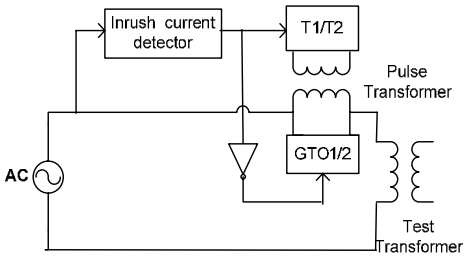

Fig. 1 : Simplified one–line diagram of the inrush current compensator

When switch GTO1/GTO2 is opened the inrush current is transferred to the pulse transformer and due to the high rate of change of current a high voltage is induced across the pulse transformer. The polarity of the induced voltage is in opposition to the primary voltage

of the load transformer. This phenomenon is equivalent to injecting a flux (volt-second) into the transformer core, thus preventing flux saturation and mitigating inrush current. The magnitude of voltage induced in the pulse transformer depends on the inductance, rate of change of current and the flux. The induced voltage is limited by limiting the flux in the pulse transformer, by short circuiting the secondary of the pulse transformer by switching the anti parallel connected thyristors T1/T2. The selection of switching of T1/T2 depends on the polarity of the voltage induced on the secondary winding of pulse transformer, which in turn depends on the direction of inrush current. The polarity of inrush current is found from the polarity of dc component present in the transformer current through Fast Fourier Transform (FFT) analysis.

The flow chart of the control system of the inrush current compensator is shown in Fig.2. The controller uses the magnitude of instantaneous power for identifying inrush current from faults and other load currents. The method of detecting inrush current from faults and other load currents is based on the different behavior of the instantaneous power. The instantaneous power due to inrush current comprises of both positive and negative varying values which is exponentially decaying. For faults and load currents the instantaneous power is only positive or less negative. This feature of instantaneous power is used to distinguish the inrush current from other currents. The inputs to the multiplier are v(t)and i(t) and it computes the value of instantaneous power p(t).

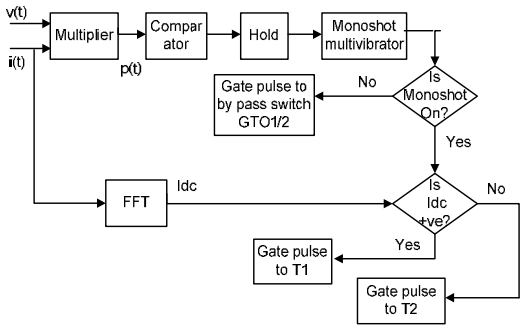

Fig. 2 : Control diagram of inrush current compensator

A comparator detects the negative value of instantaneous power, compares with a threshold value and if the threshold value is high, it generates a high digital output. This digital output is used to generate a mono shot pulse of required width which triggers the GTO1/GTO2. If the dc component of inrush current is positive, it triggers thyristor T1 and if it is negative, it triggers T2. The threshold value is the negative of the maximum instantaneous power for a transformer during inrush current which is predetermined.

IV. SIMULATION RESULTS

The effectiveness of the proposed technique is investigated by simulation on a single phase 230V/230V, 1kVA 50 Hz transformer using PSCAD. The test transformer is switched on at various inception angles against positive residual flux of 0.8pu. Residual flux is incorporated by connecting a current source in parallel with primary winding of the load transformer. Fig.3 shows the variation of inrush current and flux for a switching instant of 0.1s (0^0). First plot shows the inrush current; second plot flux and the third plot dc component. Simulations are carried for different switching angles. Table I summarizes the peak values of inrush current, flux, dc component and settling time for different switching angles. Fig.4 shows the plot of inrush current, instantaneous power and inrush current detection signal (output of monoshot). .Next the inrush current mitigation technique is applied and the transformer is again energized at different switching angles. Fig.5 shows the pot of inrush current, flux and dc

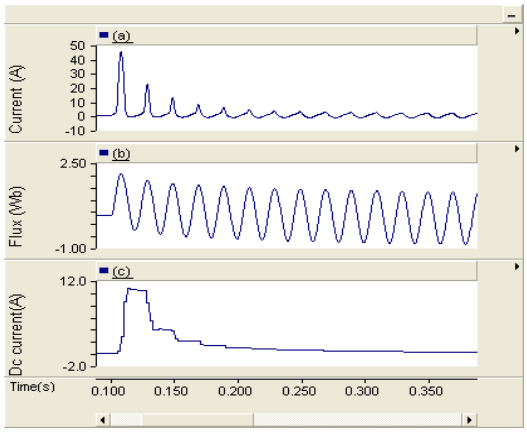

Fig. 3 : Transformer energization at switching angle 0^0 (a) Inrush currnt (b) Flux (c) DC component

TABLE I

PARAMETERS AT 0.8PU POSITIVE RESIDUAL FLUX BEFORE COMPENSATION

Switching angle		0^0	90^0	180^0	270^0
Peak current(A)	1st	45	2.7	-20	30
	2nd	26	1.2	-2.9	16
Peak DC (A)		11.2	0.14	-3.4	5
Peak Flux (pu)	1st	2.03	1.31	-1.7	1.8
	2nd	1.76	1.29	-1.35	1.5
Settling time (s)		0.9	1	0.9	1

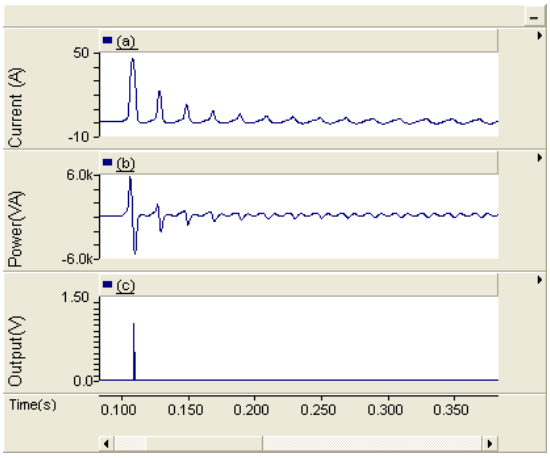

Fig. 4 : Transformer energization at switching angle 0^0 (a) Inrush current (b) Instantaneous power (c) Inrush current detection signal

component after applying the compensting technique at a switching angle of 0^0. Simulations are carried for different switching angles and the results are tabulated in Table 2. The graphs shows that the first and second

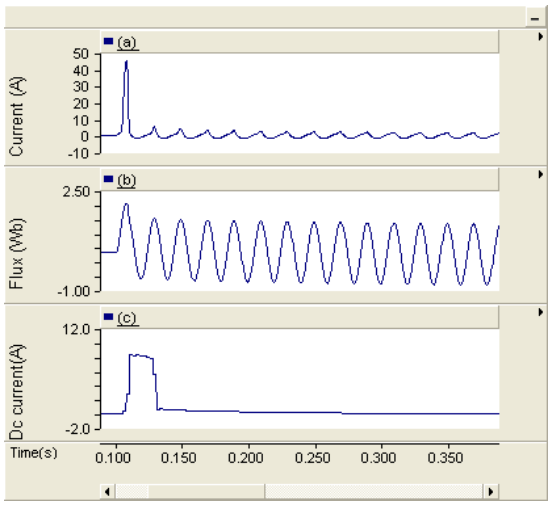

Fig. 5 : Transformer energization with compensator at switching angle 0^0(a) Inrush currnt (b) Flux (c) DC component

peak of the inrush current are 45A and 26A respectively before compensation and the current settling time is 0.9s. After the compensation there is no change in the first peak value. However second peak of inrush current is reducd to 2.4A and the settling time is reuced to 0.01s. Before compensation the value of first peak flux is 2.03pu which is highly unbalanced. After the voltage injection, there is no reduction flux for the first peak. However the second peak of flux reduced to 1.1pu from 1.76pu and flux balance is achievd at 0.11s. Ater the compensation the peak dc component is also reduced from 11A to 8.2A. As the inrush current is detected after first half cycle of energization, the dc component present is compensated wthin 0.01s after switching.

TABLE 2

PARAMETERS AT 0.8PU POSITIVE RESIDUAL FLUX AFTER COMPENSATION

Switching Angle		**0^0**	**90^0**	**180^0**	**270^0**
Peak current(A)	1^{st}	45	2.7	-9.4	30
	2^{nd}	2.4	1.2	-2.9	5.3
Peak DC (A)		8.2	0.14	-3.4	5
Peak Flux (pu)	1^{st}	2.03	1.31	-1.7	1.8
	2^{nd}	1.1	1.29	-1.4	1.5
Settling time (s)		0.01	0.01	0.01	0.01

The transition of primary current of the load transformer from GTO1 to the primary of pulse transformer during compensation is shown in Fig.6. The first plot shows the load transformer energization current through GTO1. Second plot the change over current from GTO1 to pulse transformer and third plot the transformer primary current. Transit time taken is 1ms. Due to this high rate of change of current the voltage induced in the primary winding of pulse transformer is 1748V and peak voltage induced in the primary of load transformer is 1846V. This peak voltage is limited by short circuiting the secondary of

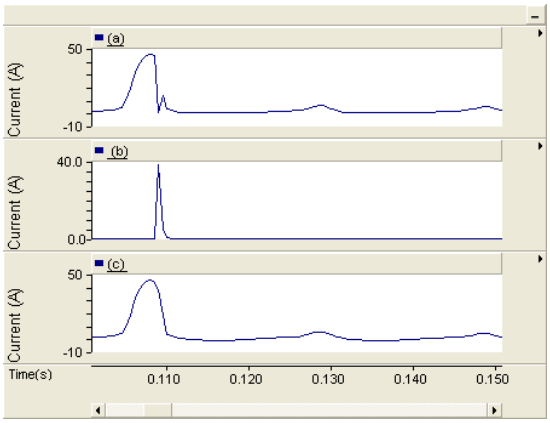

Fig. 6 : Current through a) GTO1 b) Pulse transformer c) Load transformer

the pulse transformer. The voltage seen on the primary winding and secondary winding of load transformer is 890V and 938V respectively. Fig.7 shows the variation of voltage injected by the pulse transformer and voltage on the primary side of load transformer.

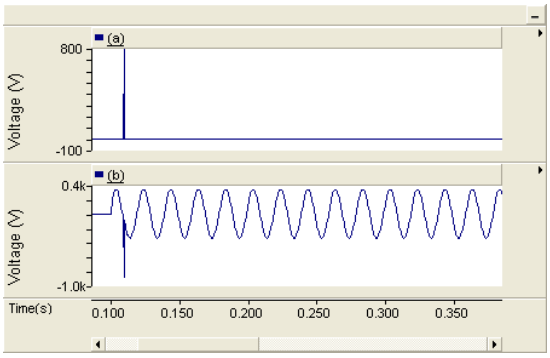

Fig. 7 : Voltage during compensation a) Pulse transformer primary b) Load transformer primary .

The flux (volt-second) injected into the load transformer core is 0.89 Wb (890V*0.001s). The peak voltage seen by the load transformer is large and since it is for a very short duration (1ms) this does not affect the power transformer performance

V. CONCLUSION

In this paper a passive cost effective method of series compensator for mitigation of inrush current in transformers during start up mode has been proposed. The proposed scheme aims at balancing flux (volt-second) asymmetry in the core during inrush current by injecting a voltage into the primary winding of load transformer through a series connected pulse transformer. The circuit for the series voltage injection and a technique to limit the injected voltage has been also proposed. This strategy on the basis of the voltage injection is quite different from present approaches of inrush current reduction. This control strategy is easy to implement because the series compensator is effective in reduction of the startup inrush current for all power-on angles without prior measurement on residual flux in transformer core. The simulation investigations reveal that the proposed approach reduces inrush current in single phase transformers. This is achieved without any complicated hardware that too without the need for a separate source.

REFERENCES

[1] S.V. Kulkarni and S.A Khaparde, Transformer Engineering: Design and Practice. New York: Marcel Dekker, 2004.

[2] Yu Cui , Sami G Abdulsalam, Shiuming Chen and Wilsun Xu “A Sequential Phase Energization Technique for Transformer Inrush Current Reduction – Part I : Simulation and Experimental Results” IEEE Transactions on Power Delivery, Vol.20 , No.2, pp 943-949, April. 2005

[3] Wilsun Xu , Sami G Abdulsalam , Yu Cui and Xian Liu “A Sequential Phase Energization Technique for Transformer Inrush Current Reduction – Part II : Theoretical Analysis and Design Guide” IEEE Transactions on Power Delivery, Vol.20, No.2 , pp 950-957, April. 2005

[4] T Haryono and Mursid Sabdullah “ Simulation Study of Transformer Inrush Current and Mitigation Method” Proceedings of the international Conferenceo on Electrical Engineering and Informatics, Institute of Technlogy Bandung, Indonesia, pp 262-265 June 17-19, 2007

[5] John H Brunke and Klaus J Frohlich “Elimination of Transformer Inrush Currents by Controlled Switching –Part I : Theoritical Considerations” IEEE Transactions on Power Deliver, Vol.16 , No.2 , pp 276-280, April. 2001

[6] John H Brunke and Klaus J Frohlich “Elimination of Transformer Inrush Currents by Controlled Switching –Part II : Application and Performance Considerations” IEEE Transactions on Power Delivery , Vol.16 , No.2 , pp 281-285, April. 2001

[7] Vincent Molcrette, Jean-Luc Kotny,Jean-Paul Swan and Jean-Francis Brudny “Reduction of inrush current in single phase Transformer usng virtual air gap technique” IEEE Transctions on Magnetics, Vol 34, No4 , pp 1192-1194, July 1998

[8] C L Cheng, C E Lin, K C Hu and Y F Hasia “Effective supression method of three-phase transformer’s inrush current “Proceedings of IEEE TENCON 2002, pp 2030-2033.

[9] Po-Tai Cheng , Wei-Ting Chen , Yu-Hsing Chen , Chia-Long Ni and Jarsun Lin “ A Transformer Inrush Mitigatin Method For Series Voltage Sag Compensators” IEEE Transactions on Power Electronics, Vol.22 , No.5 , pp 1890-1899, Sep. 2007

[10] Mojtaba Khederzadeh “Mtigation of the impact of transformer inrush current on voltage sag by TCSC” Electric Power System Research Vol 80, issue 9, pp1049-1055, Sept 2010.

[11] Nicola Chiesa and Hans Kristian Hoidalen “ Novel Approach for Reducing Transformer Inrush Currents: Laboratory Measurements, Analytical Interpretation and Simulation studies” IEEE Transactions on Power Delivery,, Vol.25, No.4 , pp 2609-2616, Oct. 2010.

[12] Juei-Lung Shyu "A novel control strategy to reduce transformer inrush currents by series compensator" IEEE PEDS 2005, pp 1283-1288

[13] Balachandran D P, Sreerama Kumar R and Shimnamol V P "A new technique for mitgation of transformer inrush current" CIRED 2007, Vienna 21-24 May 2007.

[14] Chris Fitzer Atputharajh Arulampalam, MikeBarnes and Rainer Zurowski "Mitigation of saturation in dynamic vltage restorer connection transformers" IEEE Transctions on Power Electronics, Vol.17 No.6, pp 1058-1065 Nov. 2002.

◈◈◈

Design and Simulation of Modified Auxiliary Resonant Boost Converter for Solar Energy Based Systems

K. R. Sunil Raj[1] & K. Manjunath[2]

EEE Dept., St. Joseph's College of Engineering, Chennai - 600119, India

Abstract - Solar Power Generation (SPG) is one of the main pollution free electrical power generation system. The efficiency enhancement in the solar system is a challenging task to Electrical Power Engineers (EPE). The efficiency of PV module is very low and its power output depends on solar insolation level and ambient temperature. So maximization of power output with greater efficiency is need of today's scenario. Several earlier approaches [1-4] are not providing a control strategy for efficient minimization of losses. Moreover there is great loss of power due to mismatch of source and load. Hence, to extract Maximum Power from Solar Photo-Voltaic (SPV) Panel a Maximum Power Point Tracking MPPT system needs to be developed. This project proposes a novel soft-switching Simple Auxiliary Resonant Boost Converter (SARC) to achieve greater output from the SPV Panels. The control scheme utilizes PWM techniques to regulate the output power of boost converter at its maximum possible value. This converter is able to turn on both the active power switches at zero current and turn off at zero voltage condition to reduce the switching losses. The detailed design analysis of the SARC has been carried out and results are also validated with SIMULINK of MATLAB 2008a software. The results are comparable with earlier approaches [3, 4]. Hence this modified auxiliary boost converter is suitable for maximisation of energy output in solar power systems.

Keywords - *Resonant Converter, Solar Photo-Voltaic panel, Zero-Current Switching, Zero-Voltage Switching, Pulse Width Modulation techniques.*

I. INTRODUCTION

The limited available conventional resources of electrical energy force the electrical engineers to utilize the non-conventional energy resources for Electrical Power Generation. Non-conventional energy sources like wind, bio power, solar energy, tidal power generation are used effectively. Solar energy is one of the abundantly available non-conventional sources of energy for Electrical Power Generation (EPG). Solar cells helps to convert solar energy or photo voltaic energy to electrical energy and the output obtained from the photo voltaic system is used to meet the power requirements of the load.

The dc–dc converter for a PV system has to control the variation of the maximum power point of the solar cell output. Switch-mode power supplies utilization with higher switching frequency leads to increased periodic losses during turn-on/off [2-4]. As a result, this loss brings increasing loss of whole system. Therefore, to reduce these switching losses, a soft-switching method is proposed for this project. This Soft-switching Auxiliary Resonant Boost Converter (SARC) has better efficiency than a conventional boost converter [2, 3, 4]. Moreover, this proposed converter also boosts the low output voltage of the solar cell to the required rated voltage of the load.

II. CHARACTERISTICS OF SOLAR CELL AND MODULE

The Equivalent Circuit and its current and Voltage characteristic is shown in fig2.1, 2.2.

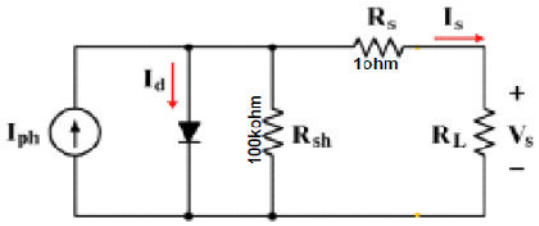

Fig 2.1: Equivalent Circuit of the Solar Cell

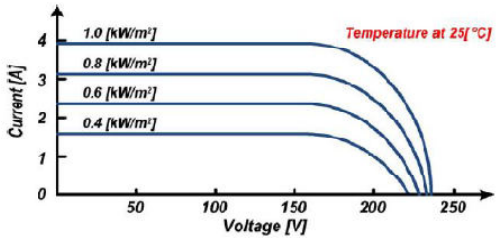

(a)

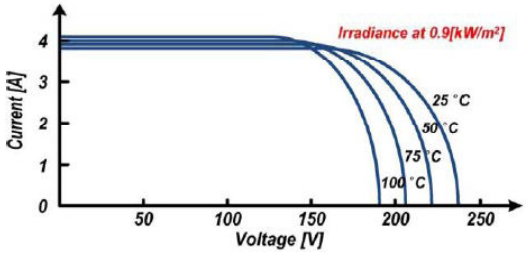

(b)

Fig. 2.2 : *I–V* Characteristic of Solar Cell.

The equivalent circuit of the solar cell [5,6,7] is composed of the internal serial resistance (Rs) and the shunt resistance (Rsh) of the diode. The output characteristics of the solar cell depend on the irradiance and the operating temperature of the cell. The solar cell output characteristics are expressed as

$$I_s = I_{Ph} - I_{sat}\left[exp\left(\frac{q(\hat{V}_s + I_s R_s)}{AKT}\right) - 1\right] - \frac{V_s + \hat{I}_s R_s}{R_{sh}} \quad (1)$$

In this equation (1), it is assumed that Rs = 0, Rsh = ∞; thus, the equation can be simplified as

$$I_s = I_{Ph} - I_{sat}\left[exp\left(\frac{qV_s}{AKT}\right) - 1\right] \quad (2)$$

Irradiance and operating temperature are important factors influencing the solar cell characteristics. If irradiance increases, the fluctuation of the open-circuit voltage is very little. However, the short circuit current has sharp fluctuations with respect to irradiance. However, for a rising operating temperature, the variation of the short-circuit current is decreased, and the open-circuit voltage is decreased in a nonlinear fashion. The Photo-Voltaic panel rating is 24V,48W.

III. MODIFIED SIMPLE AUXILIARY RESONANT CONVERTER.

A. Basic block diagram of proposed circuit

The basic block diagram of solar panel with control circuit is shown in the fig 3.1. The DC source may be Battery or Solar Cell. It converts low voltage dc supply to high voltage DC supply, and the output voltage can be controlled by controlling the duty cycle of the converter. The Simple Auxilary Resonant Circuit is used to reduce the voltgae stress and switching losses. It is also used to improve the system performance.The DC output votlage can be used to run the pump motor of water springler for agricultural irrigation systems, battery charging and also can be used for telecommunication system applications. Micro controller help to generate necessary gating pulses for MOSFETS of main power cirucit.

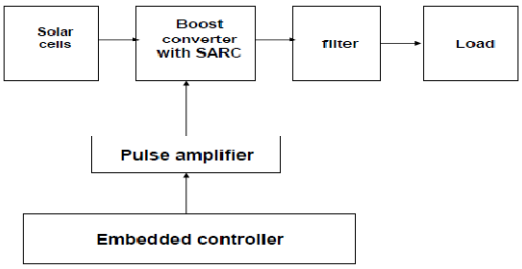

Fig. 3.1 : Basic block diagram of SARC

B. Simple Auxiliary Resonant Converter Circuit

The Simple Auxiliary Resonant converter circuit is shown in the fig 3.2. The auxiliary circuit is composed of an auxiliary switch (*S*2), a resonant capacitor (Cr), a resonant inductor (Lr), and two diodes (*D*1 and *D*2).

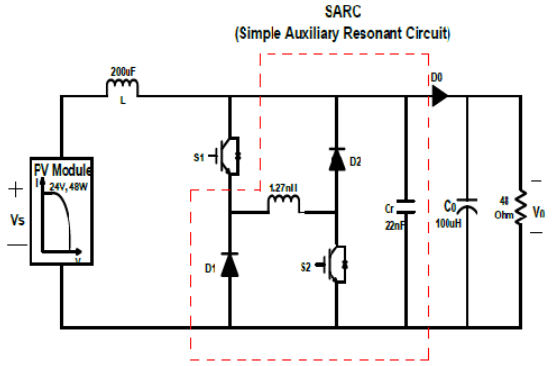

Fig 3.2 simple auxiliary resonant converter circuit

C. Modes of Operation

The operational principle of SARC has been divided into six intervals. The following assumptions are made to carry out the mode wise analysis:

1. All switching devices and passive elements are ideal.
2. Parasitic components of all switching devices and elements are negligible.
3. The input voltage (Vs) varies between 0 to 24 V.
4. This converter operates the continuous conduction mode at all intervals.

Mode 1: Operation.

The circuit diagram and waveform of Mode-1 is shown in the fig 3.3. Switches S1 and S2 are both in the OFF state, the current cannot flow through switches S1 and S2, and the accumulated energy of the main inductor is transferred to the load. In this interval, the

main inductor current decreases linearly. During this time, the current does not flow through the resonant inductor, and the resonant capacitor is charged to the output voltage.

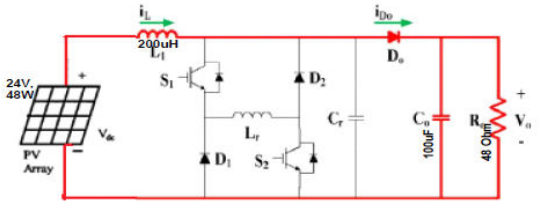

Fig. 3.3: Mode 1 Operation

$$V_L(t) = V_s - V_o$$
$$i_L(t) = i_L(t_0) - \frac{V_o - V_s}{L}t$$
$$i_{D_o}(t) = i_L(t)$$
$$i_{L_r}(t) = 0$$
$$V_{c_r}(t) = V_0$$

Mode 2: Operation.

The circuit diagram and waveform of Mode-2 is shown in the fig 3.4. After turning on switches S1 and S2, the current flows to the resonant inductor. At that time, two of the switches are turned on under zero-current condition. This is known as zero-current switching (ZCS).Because the main and auxiliary switches implement ZCS, this converter has lower switch loss than the conventional hard switching converter.

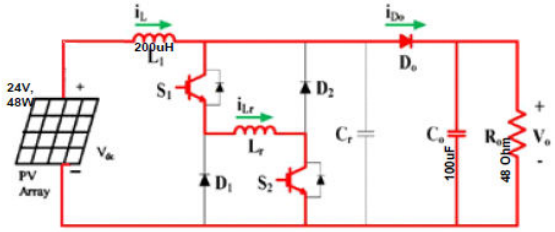

Fig. 3.4 : Mode 2 Operation

$$i_{L_r}(t_1) = 0 \qquad V_{L_r}(t) = V_0$$
$$i_{L_r}(t) = \frac{V_0}{L_r}t$$
$$i_L(t) = i_L(t_1) - \frac{V_0 - V_s}{L}t$$
$$i_L(t_2) = i_{L_r}(t_2)$$
$$i_{D_o}(t_2) = 0$$

Mode 3: Operation.

The circuit diagram and waveform of Mode-3 is shown in the fig 3.5. The current that was flowing through the load and also through output diode Do now no longer flows, since *t*2 and the resonant capacitor Cr, and the resonant inductor Lr start a resonance. The current flowing to the resonant inductor is a combination of the main inductor current and the resonant capacitor current.

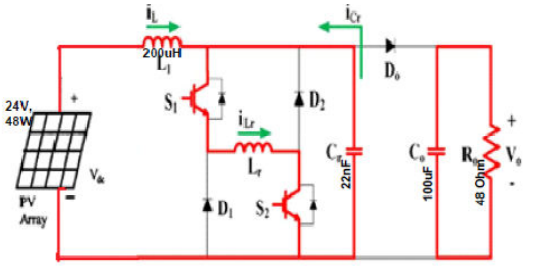

Fig. 3.5: Mode 3 Operation

$$i_L(t) = i_L(min) + i_{c_r}$$
$$V_{c_r} = \frac{1}{c}\int i_{c_r}\,dt$$
$$V_{c_r}(t) = V_0 \cos \omega_r t$$
$$i_{c_r} = \frac{V_0}{z_r}\sin \omega_r t$$
$$i_L(t) = i_L(min) + \frac{V_0}{z_r}\sin \omega_r t$$
$$V_{c_r}(t_2) = V_0$$
$$V_{c_r}(t_3) = 0$$

Mode 4: Operation.

The circuit diagram and waveform of Mode-4 is shown in the fig 3.6.In this interval, the freewheeling diodes of D1 and D2 are turned on, and the current of the resonant inductor is the maximum value. The resonant inductor current flows to the freewheeling diodes S1−Lr−D2 and S2−Lr−D1 along the freewheeling path. During this time, the main inductor voltage equals the input voltage, and the current accumulating energy increases linearly.

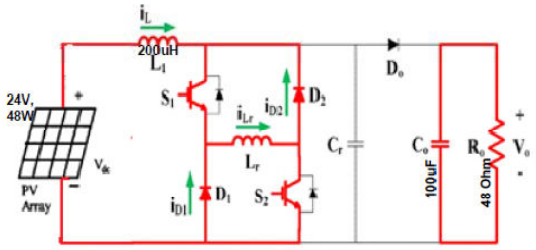

Fig. 3.6: Mode 4 Operation

Mode 5: Operation.

The circuit diagram and waveform of Mode-5 is shown in the fig 3.7. In interval 5, all of switches are turned off under the zero voltage condition by the resonant capacitor. When all of the switches are turned off, the resonant capacitor Cr is charged to the output voltage by two of the inductor currents. Until the resonant capacitor

has been charged to Vo, the output diode is in the OFF state.

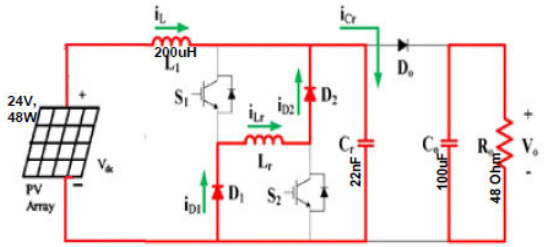

Fig. 3.7: Mode 5 Operation

$$V_{C_r}(t_4) = 0$$
$$i_L(t) = I_{max}$$
$$i_{L_r}(t) = I_{max} - (I_{max} + I_{L_{r\,max}}) \cos \omega_r t$$
$$V_{C_r}(t) = Z_r (I_{max} + I_{L_{r\,max}}) \sin \omega_r t$$
$$V_{C_r}(t_5) = V_o$$

Mode 6: Operation.

The circuit diagram and waveform of Mode-6 is shown in the fig 3.8.When the resonant capacitor equals the output voltage, and the output diode is turned on under the zero voltage condition. During this interval, the main inductor current IL and the resonant inductor current ILR flow to the output through the output diode D0. At that time, two of the inductor currents are linearly decreased, and the energy of the resonant inductor is completely transferred to the load. Then, the interval 6 is over.

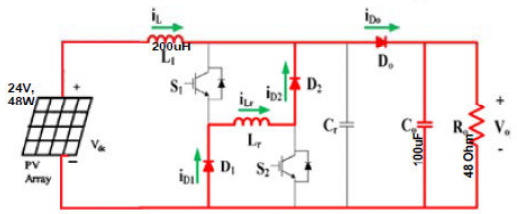

Fig. 3.8 : Mode 6 Operation

$$i_{D_o}(t) = i_L(t) + i_{L_r}(t)$$
$$i_{L_r}(t_5) = (I_{max} + I_{L_{r\,max}}) * \cos \omega_r (t_5 - t_4) t - I_{max}$$
$$V_{C_r}(t) = V_o$$
$$i_L(t) = I_{max} - \frac{V_o - V_s}{L_r} t$$
$$i_{L_r}(t) = i_{L_r}(t_6) - \frac{V_o}{L_r} t$$
$$i_{L_r}(t_6) = 0$$

The various modes of operation with equivalent circuit are explained. Corresponding waveforms are shown in Fig 3.9.

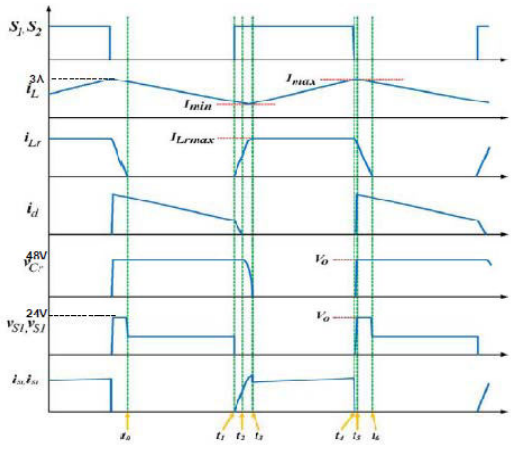

Fig 3.9: Waveform for Modes Operation

IV. DESIGN SIMPLE AUXILIARY RESONANT CONVERTER

The design of simple boost converter is presented below.

Input voltage	V_{in} = 24V
Switching frequency	f_s = 30KHZ
ON time	T_{on} = 16.66µs
Output power	P_o = 48W

Design calculations for duty ratio:

The design calculations for duty ratio is presented below

Duty ratio $$K = \frac{T_{on}}{T} = \frac{33.33 * 10^{-6} * 0.5}{33.33 * 10^{-6}} = 0.5$$

Design calculations for output voltage:

The design calculations for output voltage is presented below

Output Voltage $$V_a = \frac{V_s}{1-K} = \frac{24}{1-0.5} = 48V$$

Design calculations for output current:

The design calculations for output current is presented below

Output current $$I_a = \frac{V_a}{R_a} = 1A$$

Design calculations for output power:

The design calculations for output power is presented below

Output power $P_o = V_a * I_a = 48 * 1 = 48W$

Design calculations for Load resistance:

The design calculations for Load resistance is presented below

Load resistance $R_o = \frac{V_o^2}{P_o} = \frac{48^2}{48} = 48\Omega$

Design calculations for Inductance:

The design calculations for Inductance is presented below.

Inductance

$$L = \frac{K(1-K)*R}{2F} = \frac{.5(1-.5)*48}{2*30*10^3} = 200*10^{-6} \text{ H}$$

V. SIMULATION OF SIMPLE AUXILARY RESONANT CONVERTER

The simple auxiliary resonant converter circuit diagram are shown in the fig 5.1 the output results are obtained below.

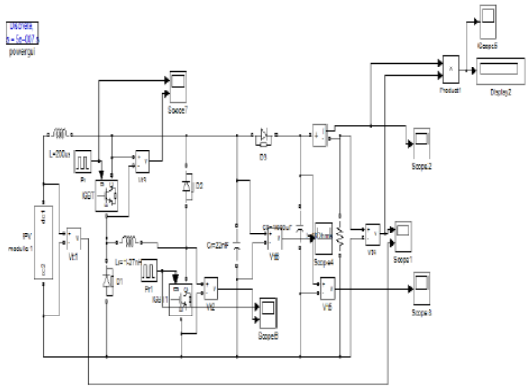

Fig. 5.1 : Simple auxiliary resonant converter simulation Diagram

A. Simple Auxiliary Resonant Converter Circuit Performance Results

The input voltage (24V) waveform of the Simple Auxiliary Resonant Converter circuit is shown in the fig 5.2. The waveform of VG and VDS across S1and S2 of the proposed circuit is shown in fig 5.3 and 5.4. The switch voltage is zero when the switches are turned ON and the output current waveform of the proposed circuit is 1A as shown in the fig 5.5. The output voltage and power waveforms of the proposed circuit are 48V and 48W are shown in the fig 5.6 and 5.7respectively.

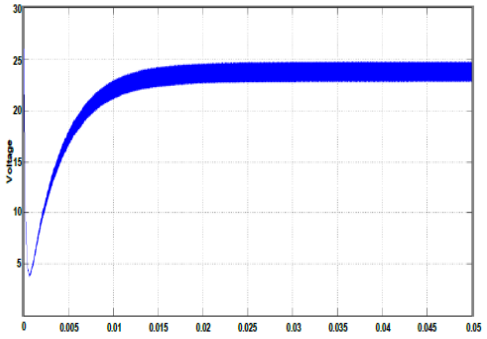

Fig 5.2 : DC input voltage waveform

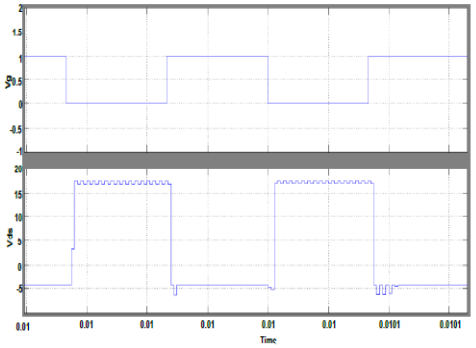

Fig 5.3 : Waveform of VG and VDS across switch 1

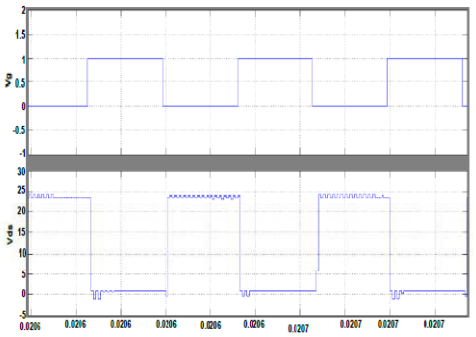

Fig 5.4 : Waveform of VG and VDS across switch 2

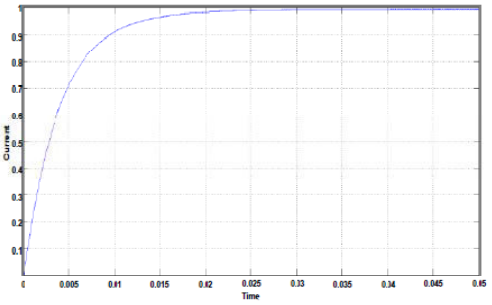

Fig 5.5 : DC output current waveform

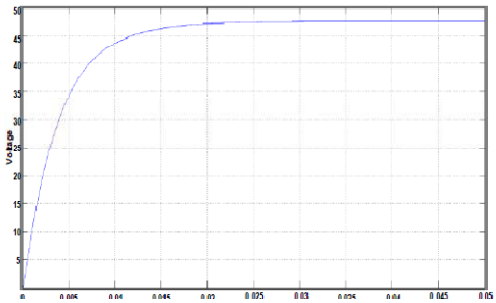

Fig 5.6 : DC output voltage waveform

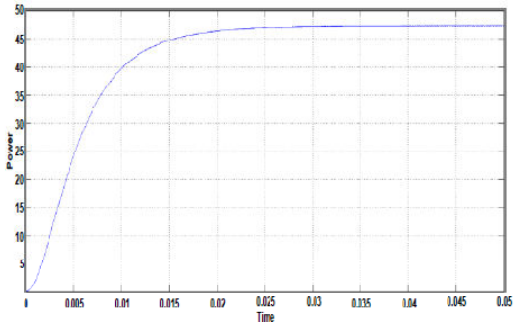

Fig 5.7 : DC output power waveform

VI. CONCLUSION

The Simple Auxiliary Resonant Boost Converter analysis and its implementation which is suitable for energy output maximization in solar power systems is presented in this paper. This soft-switching boost converter is easy to control because the two switches are controlled by the same PWM signal. All of the switching devices in this converter employ ZCS and ZVS which drastically minimizes the switching losses. The SARC simulation has been carried out using SIMULINK of MATALAB 2008a Software. The results are comparable with the earlier approaches. Hence, this soft-switching boost converter can be used in a stand-alone and a grid-connected system using a PV power conditioning system. The most commonly employable applications are water springler irrigation system, battery charging, Telecommunication etc.,

REFERENCES

[1] Sang-Hoon Park, ―Implementation of renewable energy based on soft switching boost converter with SARC" IEEE Transations onIndustrial Electronics,Vol.57, No.2,Feb 2010.

[2] Basu, S. Bollen, M.H.J. Bose Res ―A novel common power factor correction scheme for homes and offices‖ IEEE Trans. Power Delivery, Vol.50, No. 3, March 2003.

[3] Garcia, O. Cobos, J.A. Prieto, R. Alou, P. Uceda, J. Div. de Ingenieria ―Single phase power factor correction: a survey‖, IEEE Trans. Power Electronics, Vol. 18, No. 3, May 2003.

[4] K.C. Tseng, and T.J. Liang, ―Novel high-efficeincy step-up converter‖, in IEEElectric Power Appl., Vol. 151, pp. 182-190, 2004.

[5] Power Electronics, Muhammad H. Rashid.

[6] www.ieee.org

[7] www.mathwork.com

NOMENCLATURE

i_{s1}	Main switch current.
i_{s2}	Auxiliary switch current.
i_L	Main inductor current.
i_{Lr}	esonant inductor current.
I_{min}	Minimum current of the main inductor.
I_{max}	Maximum current of the main inductor.
$I_{Lr,max}$	Maximum current of the resonant inductor.
Δ_{iL}	Current ripple of the main inductor.
$V_{S,\min}$	Minimum output voltage of the solar cell.
$V_{S,\max}$	Maximum output voltage of the solar cell.
V_L	Main inductor voltage.
V_{Lr}	Resonant inductor voltage.
V_{Cr}	Resonant capacitor voltage.
V_{FW}	Freewheeling voltage drop.

◈◈◈

Investigation on Doubly Fed Induction Generator Steady State Parameters

Sunil Kumar, Nitin Goel & P.R. Sharma

EEE Deptt., YMCA University of Science & Technology. Faridabad, India

Abstract - In this paper steady state characteristic of a variable speed Doubly fed induction generator (DFIG) is investigated. Torque and speed is used as design parameters for DFIG. From mathematical model it is found that on increase of rotor injection voltage and resistance, the torque speed response is shifted from over synchronous to sub synchronous range. The stability of DFIG operation is entirely dependent on torque. The functional relationship of generator further validated using MATLAB and experimental model. DFIG find application mainly in wind energy conversion system.

Keywords - *Asynchronous Operation, Doubly fed induction generator (DFIG), Rotor resistance, Wind energy.*

I. INTRODUCTION

The growing demand of energy in industrialized world and environmental problems determined some important decision at political level that consider even more important to improve the percentage of energy produced by renewable sources[1]. A lot of efforts are devoted to increase the efficiency of the generation systems based on wind, sun, hydro and biomass.

Wind power is one of the most interesting technologies, especially considering the developments in the last decade. The electrical energy generation by wind depends on different factors, in particular the wind speed and the characteristics of the wind turbine generator [2]. There are different technical solutions that have been set up for different cases, for wind turbines in a range from less 1 kW to as large as 3 MW or more, to obtain the maximum efficiency and reliability. Traditionally the wind power generation has used fixed speed induction generators that represent a simple and robust solution, and then variable speed turbines have been considered. The advantages of variable speed turbines is that they provide higher energy, allow an extended control of both active and reactive power and present less fluctuation in output power.

Both induction and synchronous generators can be used for wind turbine systems. Induction generators can be used in a fixed speed system or a variable-speed system, while synchronous generators are normally used in power electronic interfaced variable-speed systems. Mainly, three types of induction generators are used in wind power conversion systems: cage rotor, wound rotor with slip control by changing rotor resistance, and DFIG [6]. The cage rotor induction machine can be directly connected into an ac system and operates at a fixed speed or uses a full-rated power electronic system to operate at variable speed. The wound rotor generator with rotor resistance- slip control is normally directly connected to an ac system, but the slip control provides the ability of changing the operation speed in a certain range. The DFIG provides a wide range of speed variation depending on the size of power electronic converter systems. In this paper we discuss the systems without power electronics.

Doubly-fed induction machines can be operated as a generator as well as a motor in both sub synchronous and super synchronous speeds, thus giving four possible operating modes. Only the two generating modes at sub synchronous and super synchronous speeds are of interest for wind power generation. In a DIFG the slip rings are making the electrical connection to the rotor [3-4]. If the generator is running super-synchronously, electrical power is delivered to the grid through both the rotor and the stator. If the generator is running sub-synchronously, electrical power is delivered into the rotor from the grid.

II. STEADY STATE ANALYSIS OF DOUBLY FED INDUCTION GENERATOR

The steady state performance can be described by using equivalent circuit model shown in fig. 2.1[5],

where motor convention is used. In this figure, V_S and V_R are the stator and rotor voltages, I_S and I_R are the stator and rotor current, R_S and R_R are the stator and rotor resistance, X_S and X_R are the stator and rotor leakage reactance, X_M is the magnetizing reactance and s is slip.

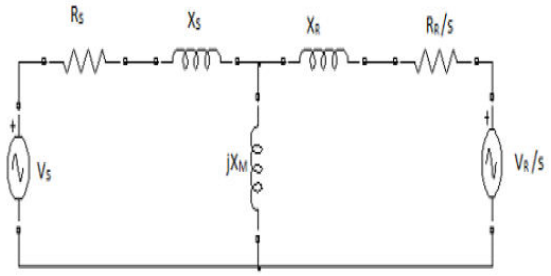

Fig. 2.1 : DFIG equivalent circuit with injected rotor voltage

The rotor current (I_R) can be calculated from

$$I_R = \frac{V_S - \frac{V_R}{s}}{(R_S + \frac{R_R}{s}) + j(X_S + X_R)} \quad (1)$$

The torque (T) of the machine which equates to the power balance across the stator to rotor gap can be

$$T = I_R{}^2 \frac{R_R}{s} + \frac{P_R}{s} \quad (2)$$

Where the power supplied or absorbed by

$$P_R = \frac{V_R}{s} I_R \cos\theta$$

$$P_R = Re(\frac{V_R}{s} I_R^*) \quad (3)$$

where $I_R{}^*$ is active rotor current

III. STEADY STATE CHARACTERISTICS OF DOUBLY FED INDUCTION GENERATOR

It is a way to investigate of operating regularities of DFIG characteristic curves through simulation. Typical characteristic curves of a DFIG are torque versus speed and real power versus speed characteristics. In induction machine those characteristics depend on the injected rotor voltage in addition to applied stator voltage.

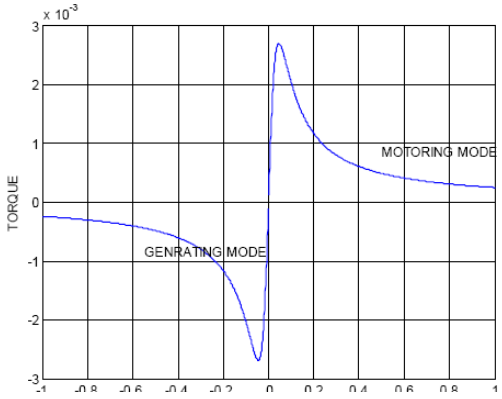

Fig. 3.1: Torque speed characteristics of DFIM

A conventional fixed-speed induction machine operates in generating mode for -1< s ≤0 and motoring mode for 0< s ≤1. Fixed-speed induction machine, a DFIM can run both over and below the synchronous speed to generate electricity. Fig.3.1 shows a simulated DFIM torque-speed characteristic for an injected rotor voltage as the operating slip varies from s=-1 to s = 1. It can be seen from Fig.3.1, the DFIM generating mode, corresponding to the negative torque values can extend from negative slip (super synchronous speed) to positive slip (sub synchronous speed).

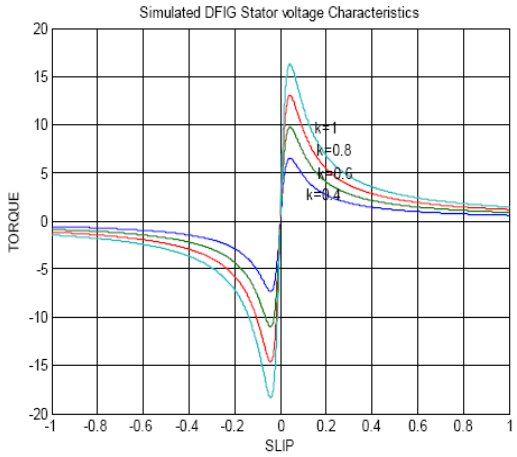

Fig. 3.2 : Simulated DFIG Stator Voltage Characteristics

The torque is proportional to the square of the stator supply voltage and a reduction in stator voltage can produce a reduction factor in speed voltage. Fig.3.2 shows torque speed characteristics for various value of reduction factor (k).

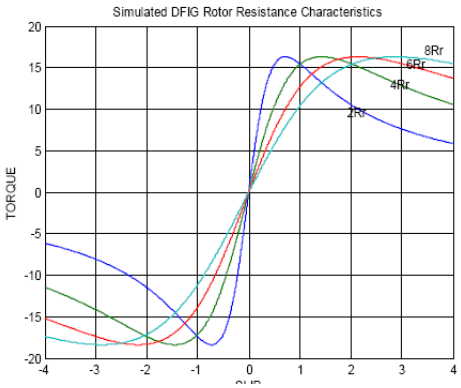

Fig. 3.3 : Simulated DFIG Rotor Resistance Characteristics

The slip at maximum torque is directly proportional to rotor resistance R_r but the value of torque is independent of R_r. When R_r is increased by inserting external resistance in the rotor of a wound rotor motor, the torque is unaffected but the speed at which it occurs can be directly controlled. The results are shown in fig.3.3.

Fig.3.4 shows the real power as V_q increased from 0.2 to 0.6pu while V_d is kept constant at 0pu.

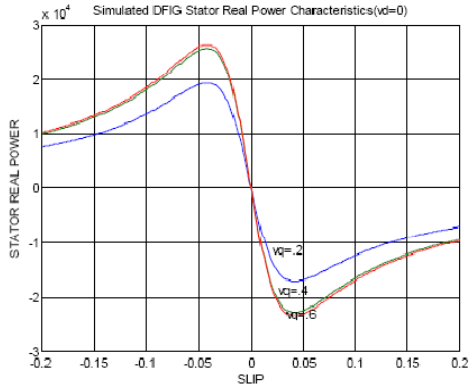

Fig. 3.4 : Simulated DFIG Stator Real Power Characteristics (V_d =0)

Examining these curves reveals the following:

- Either V_q or V_d component of the rotor injected voltage increases positively, the DFIG real power generation characteristics shifts more into sub synchronous speed range.
- V_q or V_d increases positively, the generation pushover power of a DFIG rises too, showing increased DFIG stability and power generation capability.
- V_d changes from negative to positive, DFIG real power changes gradually from flowing into (motoring) to flowing out of (generating) the induction machine.

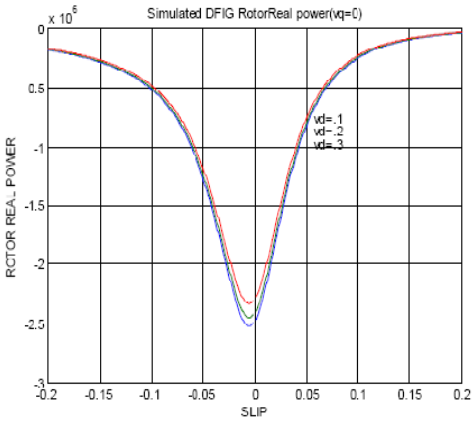

Fig. 3.5 : Simulated DFIG Rotor Real Power Characteristics (V_q=0)

Fig.3.5 shows the real power as V_d increased from 0.1 to 0.3pu while V_q is kept constant at 0 pu. Examining these curves reveals the following:

- For both motoring and generating modes, the DFIG sends an additional real power through its rotor as shown in Fig. 3.5.
- For high values of the injected rotor voltage, the real power delivered to the DFIG rotor is maximum at synchronous speed at which the DFIG rotor is equivalent to a short circuit. A proper control of Vq and Vd is essential to prevent high currents flowing in the rotor.

IV. CONCLUSION

From the simulation analysis it is concluded that the DFIG characteristics are affected by its injected rotor voltage. Within variation in amplitude of the rotor injected voltage, the DFIG torque speed characteristics are shifted from over synchronous to sub synchronous speed range to generate electricity. It also increases the DFIG pushover torque, thereby improving the stability of operation. With increase in rotor injected voltage, the pushover power of the DFIG rises.

REFERENCES

[1] Ahmad M. Alkandari, Soliman Abd-Elhady Soliman, Mansour H. Abdel-Rahman, "Steady State Analysis of a Doubly Fed Induction Generator", energy and power engineering,vol.3, pp. 393-400, Sept.2011.

[2] L.Piegari, R.Rizzo and P.Trricoli, "High Efficiency Wind Generator with Variable Speed Dual Excited Synchronous Machine", International Conference on Clean Electrical Power 2007, Capri, pp. 795-800, 21-23 May 2007.

[3] Ekanayake, J. E., "Dynamic Modeling of Doubly Fed Induction Generator Wind Turbines", IEEE Transactions on Power Systems, vol. 18, pp. 803-809, May 2003.

[4] Sharma Pawan, Bhatti Tricholen Singh, Ramakrishana Kondapi Seha Srinivasa "Doubly Fed Induction Generator: an Overview", Journal of Electrical and Electronics Engineering, vol. 3, pp.189-194, Oct 2010.

[5] Olimpo Anaya Lara, Nick Jenkins, "Wind Energy Generation – Modeling and Control". Wiley, 2009.

[6] F. Blaabjerg and Z.Chen "Power Electronics for Modern Wind Turbine", Morgan & Claypool Publisher, San Rafael, 2006.

APPENDIX

0.37KW, Rated Voltage 380V, Rated Current 1.2A

R_S (Stator Resistance) 0.083pu

X_S (Stator Reactance) 0.1055pu

R_R (Rotor Resistance referred to Stator side) 0.587pu

X_R (Rotor Reactance referred to Stator side) 1.285pu

X_M (Magnetizing Reactance) 0.0032 pu

Frequency 50 HZ

◈◈◈

Comparison of Varies Method for Energy Harvesting System from Piezoelectric Material

Milind S. Burle & Vyankateshwar.G. Girhepunje

Dept. of Electronics & Communication, Priyandarshani College of Engineering, Nagpur, India

Abstract - Now a day, increasing demand for lowpower and portable-energy sources due to the development and mass consumption of portable electronic devices. Energy harvesting (also known as power harvesting or energy scavenging) is derived from external sources (e.g., solar power, thermal energy, wind energy, biomechanical energy and vibration environment), captured, and stored. Piezoelectric material has the ability to be used as mechanism to transform mechanical and biomechanical energy, like ambient vibration and human motion, to electrical energy. In this paper compare varies method for energy harvesting system from piezoelectric material. 1) energy harvesting system based on the enhanced synchronized switching technique**.** 2) self-tunable piezoelectric vibration energy harvesting system 3) cantilever-based energy harvesting devices (EHD) 4) use of piezoelectric polymers in order to harvest energy from people walking and the fabrication of a shoe capable of generating and accumulating the energy.

Keywords - *Micro-generator, piezoelectric generator, shoe Energy generator, PVDF film.*

I. INTRODUCTION

Energy harvesters provide a very small amount of power for low-energy electronics. While the input fuel to some large-scale generation costs money (oil, coal, etc.), the energy source for energy harvesters is present as ambient background and is free. For example, temperature gradients exist from the operation of a combustion engine and in urban areas, there is a large amount of electromagnetic energy in the environment because of radio and television broadcasting. Energy harvesting devices converting ambient energy into electrical energy have attracted Much interest in both the military and commercial sectors. Some systems convert motion, such as that of ocean waves, into electricity to be used by oceanographic monitoring sensors for autonomous operation. Future applications may include high power output devices (or arrays of such devices) deployed at remote locations to serve as reliable power stations for large systems. Another application is in wearable electronics, where energy harvesting devices can power or recharge cell-phones, mobile computers, radio Comm .equipment, etc. All of these devices must be sufficiently robust to endure long-term exposure to hostile Environments and have a broad range of dynamic sensitivity to exploit the entire spectrum of wave motions. Piezoelectric material has the ability to be used as mechanism to transform mechanical and biomechanical energy, like ambient vibration and human motion, to power other devices [1]. The piezoelectric effect is understood as the linear electromechanical interaction between the mechanical and the electrical state in crystalline materials with no inversion symmetry.[2] The nature of the piezoelectric effect is closely related to the occurrence of electric dipole moments in solids. The latter may either be induced for ions on crystal lattice sites with asymmetric charge surroundings (as in BaTiO3 and PZTs) or may directly be carried by molecular groups. The dipole density or polarization may easily be calculated for crystals by summing up the dipole moments per volume of the crystallographic unit cell.[3]

II. MOTIVATION

As the consumer demand on body worn electronics (eg. Mobile phones, pagers, PDA's) continually increases, the multiple battery power supplies needed for microelectronics are becoming cumbersome and costly. As the power demands of microelectronics decreases the reliance of consumer electronics on the battery maybe becoming outdated. Idle microelectronic systems continually drain power unnecessarily from power supplies, unless physically disconnected, over long periods power drain on batteries make this traditional solution unreliable It has been proven in previous studies conducted by the Massachusetts Institute of Technology (MIT), that the everyday activity of walking is one such place where large

amounts of energy are expended, up to 67 watts per step for a 68 kg person. Harvesting a small amount of this energy via a suitably selected transducer would be enough to power a variety of small electronic devices.

III. PEIZOELECTRICAL PRINCIPAL

To gain energy from natural resources requires a media to transform the energy to electricity. Generally, in harvesting energy from biomechanical, there are four main methods in converting mechanical energy to electrical current or voltages which are piezoelectric actuation, electrostatic actuation, electro-active polymers and magnetic actuation. Piezoelectric and electro-active polymers are shown to have similar characteristics which are having high impedance, sharp output voltage, and very low energy conversion efficiency. Piezoelectric actuation seems more flexible in order to harvest energy from biomechanical (human motion) and ambient vibration. Thus, it has been chosen as method of harvesting energy throughout the study.

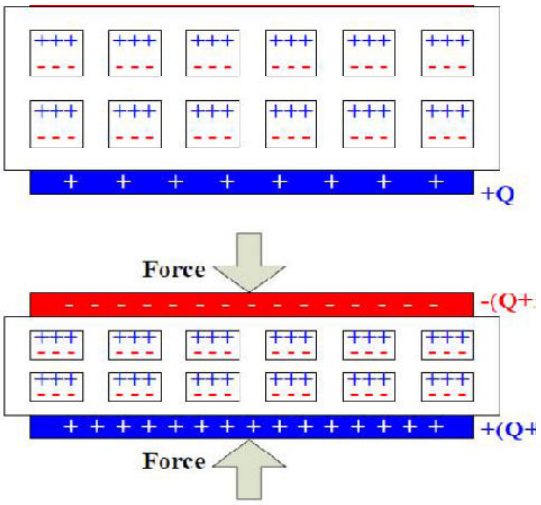

Fig. 1: Schematic of electret structure and piezoelectricity

Several methods are use for energy harvesting from piezo-electrical material. They are shown below.

A) Energy Harvesting System Based On The Enhanced Synchronized Switching Technique.

Figure 2 shows a structural vibration system consisting of a cantilever beam, a piezoelectric transducer, an electromagnet, and a rigid base. The piezoelectric element is bonded at the root of the beam. When the beam is excited by the electromagnet, a large strain is induced on the piezoelectric transducer, and an AC voltage is generated between its electrodes. Different external circuits are connected to the piezoelectric transducer to construct a passive vibration system. In a mechanical point of view, the energy harvesting process leads to the mechanical damping effect when the system is driven by a constant amplitude external force.

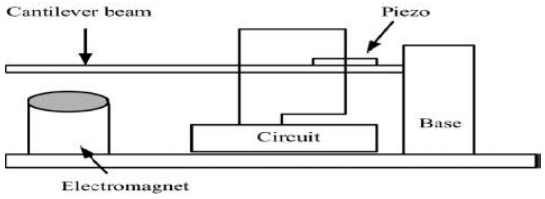

Fig. 2 : A structural vibration system with a piezoelectric Transducer

The principle of the enhanced synchronized switching harvesting (ESSH) technique is shown in Fig. 3, which includes two parts. The first one includes the piezoelectric element, the switch S1, the inductor *L*1, the diode bridge rectifier (D1-D4), and the intermediate capacitor *Cint*. The part corresponds to the interface circuit of the series SSHI proposed by Taylor et al. and described in [4,5]. The second part consists of the switch S2, the inductor *L*2 and the diode D5, which is a buck-boost static converter [4,6].

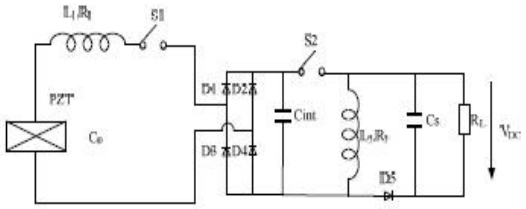

Fig. 3 : Energy extraction circuit

When the voltage of piezoelectric element reach the extreme, the switch S1 is closed for a brief time period. At the same time, there is an energy transfer from the piezo element to the intermediate capacitor *Cint* through the inductor *L*1 and the diode bridge rectifier. When the energy transfer is complete (maximal amount of charge on the capacitor *Cint*, the current is null), the switch S1 is opened. The buck-boost static converter principle consists in removing periodically the electric charge accumulated on the intermediate capacitor *Cint.* Compared with the DSSH technique [6], the control law for the switch S2 in the ESSH technique is different. When the voltage of the intermediate capacitor *Cint* increases beyond the preset voltage *VH*, the switch S2 is closed. Thus the electrical energy stored on the intermediate capacitor *Cint* is then transferred into the inductor *L*2. When the electric charge is mostly removed from the intermediate capacitor *Cint* (the voltage of the intermediate capacitor *Cint* drops down the preset

voltage *VL*), the switch S2 is re-opened and the energy stored to the inductor *L*2 is transferred to the smoothing capacitor Cs through the diode D5.

B) Self-Tunable Piezo Electric Vibration Energy Harvesting System

The electrodes of the 100 µm thick single-layers are structured with a pulsed Nd:YAG laser. This allows assigning different functions to different parts of the piezoceramics later on. The single layers are then mounted to a stack by gluing. The stack is laser-structured again in order to obtain its final shape [7]. The structure is chosen in such a way that a part of it serves as a piezoelectric energy harvester in a bending mode, while another part is used as a linear actuator. The device used in this work consists of 2 pairs of opposed cantilever beams. The purpose of the actuator is to interconnect the tips of these opposed cantilever beams and to apply the axial preload to them. The preload will produce an additional moment in the cantilevers, which will ease or harden the deflection of the beam, depending on the direction of the linear actuation. As the additional moment directly contributes to the restoring force of the spring mass- system, the resonance frequency of the system will be shifted. The whole resonator consists of four springs in form of cantilever beams and one common seismic mass represented by the actuator. To generate an additional moment on a cantilever through a lateral arm, it is important to make sure that the deflectionlines of both beams differ as much as possible. With the arm connecting the tips of two opposed cantilever beams, this condition is met very well. Since all relevant parts of the frequency tunable generator are made from the same bulk material, a cost-efficient largescale production is possible.

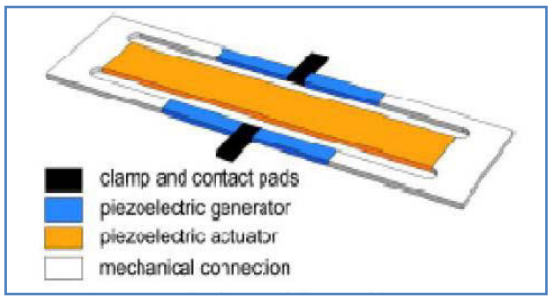

Fig 4: 3-dimensional scheme of the tunable generator

C) Cantilever-Based Energy Harvesting Devices (EHD)

The piezoelectric cantilever beam is probably the most commonly used configuration for modeling or implementing EHDs harvesting energy from vibration. Here, we have considered the bimorphs, in which two separate sheets of piezoelectric materials are bonded together, sometimes with a center shim in between them, as shown in Fig 5. An equivalent electrical circuit representation of the model is shown in Fig 6[8]

Here, On the electrical side:

V = voltage,

Cp = the capacitance of the bimorph,

R = the load resistance

On the mechanical side:

m = mass attached to the end of the cantilever beam

bm = the damping coefficient, relates stress to the tip displacement, *z*.

Y = the stiffness term, relating stress to the strain

σin = the input, in the form of mechanical vibration, is shown as a stress generator.

The dynamic model of the above system is given in as follows [6, 12]

$$\begin{bmatrix} \dot{\delta} \\ \ddot{\delta} \\ \dot{V} \end{bmatrix} = \begin{bmatrix} 0 & 1 & 0 \\ -\frac{\kappa_{sp}}{m} & -\frac{b_m b^{**}}{m} & \frac{\kappa_{sp} d}{m t_c} \\ 0 & -\frac{d Y_c r_e}{\varepsilon} & \frac{1}{RC_p} \end{bmatrix} \begin{bmatrix} \delta \\ \dot{\delta} \\ V \end{bmatrix} + \begin{bmatrix} 0 \\ b^* \\ 0 \end{bmatrix} \ddot{y}$$

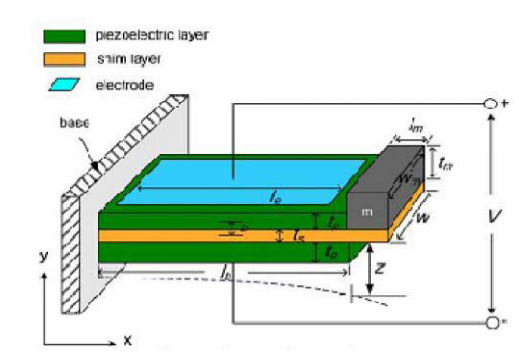

Fig. 5 : Operation of piezoelectric bimorph

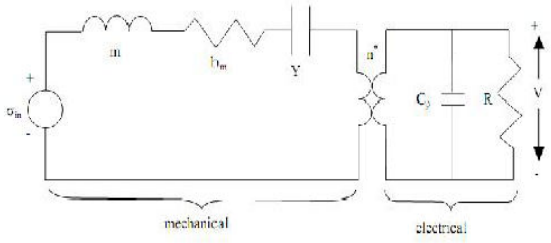

Fig. 6 : Equivalent circuit model of the piezoelectric bimorph

D) Piezoelectric Power Generator Shoe Insert

As early as 1995, Anta kiet al proposed to extract useful energy from people's ambulation to provide supplemental power for operating electrically powered artificial organs using shoe generator system made of piezoelectric ceramic transducer [9]. The piezoelectric transducer within midsole consists of a single cylindrical stack of 18 PZT ceramic slugs, each having a diameter of 0.31 inch and a thickness of 0.245 inch. The output powers of midsole generator from a man weighted 75 kg are 625, 676, and 2100 mW respectively corresponding to flat foot, heel-toe, and simulated jogging. Piezo electric materials can be characterized as either a charge or a voltage source. In the voltage mode method we model the Piezo-source as a voltage source connected in series with a pure capacitor. Voltage generated by the source is proportional to the applied stress as characterized by the following equation:

$Vo=g3nXj$ (n= 1,2,3)

g- Stress constant in a given direction

X- Applied stress

t- Film thickness

The charge generated by a Piezoelectric under stress is expressed in terms of charge density per unit area.

$D = Q/A = d3nXn$ (n= 1,2,3)

D- charge density

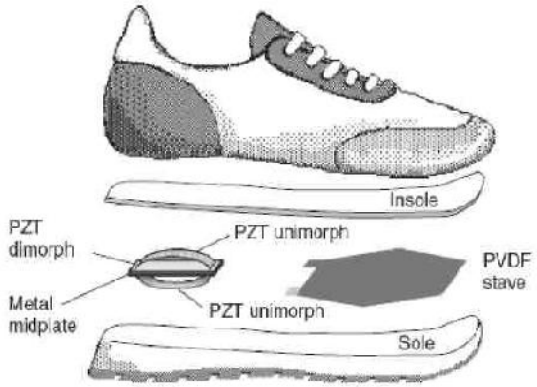

Fig. 7 : Shoe generator system.

IV. PIEZOELECTRIC MATERIAL

Piezin, the Greek word 'to press', describes Piezoelectricity as 'pressure electricity'. The Curie brothers discovered piezoelectricity in the 1880s. They found that Quartz deformed when subjected to an electric field. A Frenchman, Paul Langevin, 1916, who developed an early form of SONAR using a Quartz transmitter and receiver, created one of the first practical applications of Piezo electricity. Soon after Piezoelectric ceramics where discovered the first commercial device designed was a phonograph pickup (1947) made from Barium Titanate (BATi03). In 1955 (PZT) Lead Zirconate Titanate the most widely used piezoelectric ceramic (including its compositions) was discovered. Preceding a discovery of a small piezoelectric effect in whalebone in the 1960's researchers began an intense search into organic materials and Ferroelectric polymers. Research followed from people such as Fukada and co-workers who discovered induced surface charge in rolled films of polypeptides. A major milestone ocurred in 1969 with Kawai's discovery of a strong piezoelectric effect in, polyvinyldene fluoride (PVDF), and later (1975) its strong Pyroelectric effect. Piezoelectric materials an be categorized into three types: Ceramics- including B ATi03 (Barium Titanate), PZT (Lead Zirconium Titanate), PLZT (Lead Metaniobate), PMN (Lead Magnesium Niobate).The following comparison table lists three of the most prominent piezoelectric materials it illustrates the advantages and disadvantages inherent in each material.

PVDF FILM

The piezoelectric films used for the energy generation are constituted by a polymeric material coated in both sides by a conducting material, which form the electrodes. The polymeric material is based on the polyvinylidene fluoride (PVDF) polymer in its electroactive (β) phase. It can be processed in the form of a film by extrusion and injection or from the solution, usually in the nonelectro active α phase. In order to obtain the electroactive β phase, the α phase films must be submitted to mechanical stretching at temperatures below 100 ◦C and with a stretching ratio (ratio between the final and the initial lengths of the sample) from 4 to 7. After getting the electroactive β phase, the material must be activated by poling. This is done by subjecting the film to an electric field with amplitude larger than 60 MV/m along the thickness direction.

PZT FILM

Lead zirconate titanate also called **PZT**, is a ceramic perovskite material that shows a marked piezoelectric effect. PZT-based compounds are composed of the chemical elements lead and zirconium and the chemical compound titanate which are combined under extremely high temperatures. A mechanical filter is then used to filter out the particulates. PZT-based compounds are used in the manufacturing of ultrasound transducers, in the manufacturing of ceramic capacitors, STM/AFM actuators. acceptor doping creates *hard* PZT while donor doping creates *soft* PZT. Hard and soft PZT's generally differ in their piezoelectric constants. Piezoelectric constants are proportional to the polarization or to the electrical field generated per unit

of mechanical stress, or alternatively is the mechanical strain produced by per unit of electric field applied.

In general, *soft* PZT has a higher piezoelectric constant , but larger losses in the material due to internal friction. In *hard* PZT, domain wall motion is pinned by the impurities thereby lowering the losses in the material, but at the expense of a reduced piezoelectric constant. The dielectric constant of PZT can range from 300 to 3850 depending upon orientation and doping[10]PZT is used to make ultrasound transducers and other sensors and actuators, as well as high-value ceramic capacitors and FRAM chips. PZT is also used in the manufacture of ceramic resonators for reference timing in electronic circuitry. PZT is able to overt approximately 2.5 times more mechanical energy to electrical energy than that of PVDF film. PZT can also convert around 5 times more fore to charge than PVDF. PVDF however is 21 times more responsive to voltage generation by an applied force. The relative permittivity of PZT demonstrates that it is a much more capacitive source than PVDF since capacitance is proportional to permittivity. Due to the electro-mechanial coupling coefficient PZT is the standout material. PZT are a solid solution of lead zirconate and lead titanate, Pb(ZrxTi1-x)O3. Under a strong electric field, dipole forms because the Ti4+ or Zr4+ deviates from the neutral position which is the center of the unit cell. These electric dipoles can be reversed in an electric field. The reversion of dipoles can deform a PZT material.

Commercially, PZT ceramic was doped with either acceptor dopants, which create oxygen (anion) vacancies and generate hard PZT, or donor dopants, which create metal (cation) vacancies and generate soft PZT. The action vacancies facilitate the domain wall motion, so soft PZT has a higher piezoelectric constant, but larger loss due to internal friction. The hard PZT has a lower piezoelectric constant and also lower loss because the domain wall motion is pinned by the impurities.

Photo of PVDF stave under test

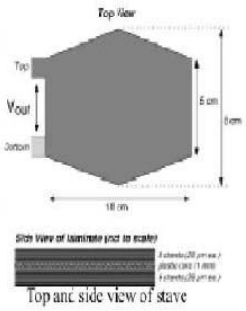

Top and side view of stave

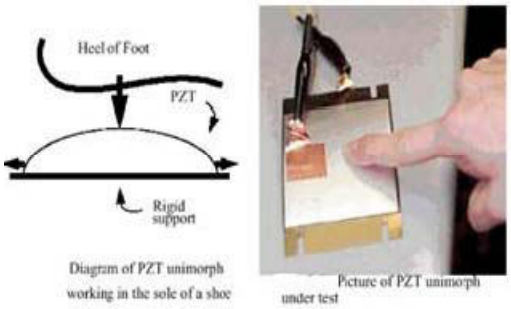

Fig. 8: Peizoelectrical film

Property	Units	PVDF	PZT
Density	10^3kg/m^3	1.78	7.5
Relative Permitivity	$\varepsilon/\varepsilon_0$	12	1200
d_{31} Constant	(10^{12})C/N	23	110
g_{11} Constant	(10^{-3})Vm/N	216	10
k_{11}constant	%At 1KHz	12	30
Acoustic Impedance	(10^6)kg/m^2-Sec	27	30

V. RESULT COMPARESION:

Energy Harvesting System Based On The Enhanced Synchronized Switching Technique

The ESSH technique proposed in the paper can be truly self-powered by using two-mode energy harvesting circuit. It consists of five sub-circuits: start-up circuit, threshold control, power manager, the control signal generator, the ESSH interface and the load. At first mode, the storage capacitor (part of the immediate capacitor *Cint*), C5, is charged by the start-up circuit using the piezoelectric element (PZT2) until enough energy is stored for supplying power for the operation of the ESSH interface. At the second mode, the ESSH interface operates and the storage capacitor, C5, is charged using the piezoelectric element (PZT1). At the same time, the piezoelectric element (PZT2) is disconnected to the start-up sub-circuit and connected to the sub-circuit of control signal generator. Threshold point that divides these two modes of operation depends on the state of charge of the storage capacitor, C5.

Self-Tunablepiezoelectric Vibration Energy Harvesting System

The system has been operated with different control strategies. With the adaptive system, the device stays resonant between 150 and 190 Hz resulting in a "resonance plateau" instead of a resonance peak. This plateau is slightly lower than the peak of the non adaptive system, as some power is deviated to the control-unit. The power consumption of the tuning mechanism can be broken down to the different tasks performed by the system. The energy consumption for one large frequency shift (190 to 160 Hz) amounts to

266μJ. This energy is required to generate the high actuator voltage.

Cantilever-Based Energy Harvesting Devices (EHD)

The center shim material of the bimorph model is brass and its Young's modulus (GPa) is *Ysh* = 110 and the seismic mass (tungsten) density (kg/m3) *D* = 17000. The acceleration magnitude is selected as $\ddot{Y}$ =2.25 m/s2. The value of optimal load resistance R_{opt} = 23.325 kΩ) and resonant frequency (*fn = 131.2* Hz) are obtained

Piezoelectric Power Generator Shoe Insert

In an attempt to determine the best material for parasitic power harvesting it is a good method to consider a Piezofilm element as a voltage generator hence:By simple analysis of this equation we an see that the energy is proportional to the square of the voltage, hence PVDF having much higher voltage sensitivity can produe larger peak amounts of energy.When operating at low frequencies (in our case l-4Hz) it is feasible to model the source as a parallel plate capacitor.

REFERENCES

[1] Sodano, H. A., Magliula, E. A., Park, G., and Inman, D. J.,2002, "Electric Power Generation from Piezoelectric Materials," in Proceedings of the 13th International Conference on Adaptive Structures and Technologies, (2002).

[2] Gautschi, G (2002). Piezoelectric Sensorics: Force, Strain, Pressure, Acceleration and Acoustic Emission Sensors, Materials and Amplifiers.. Springer.

[3] M. Birkholz (1995). "Crystal-field induced dipoles in heteropolar crystals – II. physical significance". Z. Phys. B 96: 333–340 Bibcode1995ZPhyB..96..333Bdoi:10.1007/BF01313055.http://www.mariobirkholz.de/ZPB1995b.pdf.

[4] E. Lefeuvre, A Badel, C. Richard, L. Petit and D. Guyomar, "A comparison between several vibration-powered piezoelectric generators for standalone systems," Sensor Actuators A, vol. 126, no. 2, pp. 405-416, 2006.

[5] G. W. Taylor, J. R. Burns, S. M. Kammann, W. B. Powers and T. R. Welsh, "The energy harvesting eel: A small subsurface ocean/river power generator," IEEE J. Oceanic Eng., vol. 26, no. 4, pp. 539-547, 2001.

[6] M. Lallart, L. Garbuio, L. Petit, C. Richard and D. Guyomar, "Double Synchronized Switch Harvesting (DSSH): A New Energy Harvesting Scheme for Efficient Energy Extraction," IEEE Trans. Ultrason. Ferroelectr. Freq. Control., vol. 55, no. 10, pp. 2119-2130, 2008.

[7] Eichhorn C. et al. "A piezoelectric harvester with an integrated frequency-tuning mechanism", Technical Digest PowerMEMS 2009, (Washington, USA December 1-4, 2009) , pp. 45-48

[8] Alireza Khaligh, Peng Zeng, and Cong Zheng, "Kinetic Energy Harvesting Using Piezoelectric and Electromagnetic Technologies— State of the Art," IEEE Transactions on Industrial Electronics, vol. 57, no.3,March2010

[9] J. F. Antaki, G. E. Bertocci, E. C. Green, A. Nadeem, T. Rintoul, R. L. Kormos, and B. P. Griffith, "Gait-powered autologous battery charging system for artificial organs," ASAIO Journal, vol. 41, pp. 588-595, 1995.

[10] Piezo Technologies' Materials Specifications.

◈◈◈

Design of a Microcontroller Based PFC

Pradeep Kumar[1], P.R.Sharma[2] & Ashok Kumar[3]

[1&2]Dept. of Electrical & Electronics Engineering, YMCA University of Science & Tech., Faridabad, Haryana, India
[3]M.R International University, Faridabad, Haryana, India

Abstract - With the increasing demand for power from the ac line and more stringent limits for power quality, power factor correction has gained great attention in recent years. A variety of circuit topologies and control methods have been developed for the PFC application. International Standards in the area of compliance of a product's AC mains current harmonics have forced that new power supply design must include the power factor correction at the front end. The new trend in Power Supply is towards the digital control. This paper discusses the design of a controller for Power Factor Correction (PFC). A microcontroller based PFC design is proposed and design issues are discussed. PFC is simulated using MATLAB and results are reported. Interface requirement between the power converter and microcontroller are discussed.

Keywords - *PFC, THD, Microcontroller, PI Controller, ac-dc converter, control design.*

I. INTRODUCTION

Most of the power application consists of an AC to DC conversion stage after the AC main source. Rectified DC out put is used for later stages. Usually a filter having a large capacitance is employed for getting proper DC output. This results in discontinuous and short duration current spikes. These discontinuous spikes lead to increase in network losses, total harmonic distortion (THD).

Two factors that provide a quantitative analysis of quality of power in an electrical circuit are Power Factor (PF) and Total Harmonic Distortion (THD). Benefits from improvement of Power Factor include – Lower energy and distribution costs, Reduced Losses in electrical system during distribution, better voltage regulation and capacity enhancement.

With increasing demand in the area of AC to DC Conversion tighter regulation such as IEC61000-3-2 have come into force. Regulations have already been enacted in the EU that constricts how far load current may deviate from a pure sine in phase with the voltage for some types of loads. These regulations will likely get tighter in the future, be applied to smaller loads, and spread to other regions.

II. HARMONIC CURRENT EMISSION GUIDELINES

Increasing use of electronic devices in daily life has greatly increased the stress caused by harmonic currents on low-voltage alternating-current public mains networks. To maintain the quality of these networks, European Standard EN 60555-2 was created to set levels for harmonic currents injected by loads back on to the network.

There has, however, been much discussion about equipment classes and limits to apply to electronic equipment in general and equipment power supplies in particular. EN 60555-2 has been superseded by EN 61000-3-2 which sets some more practical rules and provides a clearer definition of equipment classes.

There are 4 different classes in the EN 61000-3-2 that have different limit values.

III. SYSTEM FOR STUDY

A Traditional PFC Boost Converter is depicted in Figure 3. DC Voltage output Vo is a constant, So the output of the voltage loop V_c is also constant. Outer voltage regulating control loop generates reference to inner current loop.

Fifure 8 depicts the converter transfer function showing both the loops for control. Following equations can be driven from the above figure:

$$i_g(s) = \frac{G_{iv}}{1+T_i} Vg(s) + \frac{G_{id}F_mH_i}{1+T_i} k_x V_c V_g(s) \quad (1)$$

$$Y(s) = \frac{i_g(s)}{v_g(s)} = \frac{G_{iv}}{1+T_i} + \frac{G_{id}F_mH_i}{1+T_i} k_x V_c \quad (2)$$

$$Y(s) = G_{ivcl} + T_{icl} k_x V_c \quad (3)$$

Where $T_i = G_{id}F_mH_ih_s$ is the loop gain transfer and

$T_{icl} = \frac{G_{id} F_m H_i}{1 + T_i}$ is the closed loop control to current transfer function.

Y(s) can be considered consisting of two components, $Y_1(s)$ and $Y_2(s)$ in parallel so –

$Y(s) = Y_1(s) + Y_2(s)$

$$Y_1(s) = G_{ivcl} = \frac{s}{V_o F_m h_s \omega_i (1 + \frac{s}{\omega_z})} \quad (4)$$

$$Y_2(s) = T_{icl} k_x V_c = \frac{k_x V_c}{h_s} = Y_{CLO} = \frac{I_g}{V_g} = \frac{P_g}{V_g^2} \quad (5)$$

Y1(s) is the closed loop voltage to current transfer function and Y2(s) is the closed loop current reference to current transfer function.

IV. AVERAGE CURRENT MODE CONTROL

Average current mode control employs a control circuit that regulates the average current (input or output) based on a control signal. For a PFC controller, this control signal is generated by the low frequency dc loop error amplifier. The current amplifier is both an integrator of the current signal and an error amplifier. It controls the waveshape regulation, while the control signal controls the dc output voltage. The output of the current amplifier is a "low frequency" error signal based on the average current in the shunt, and the control signal. This signal is compared to a sawtooth waveform from an oscillator, as is the case with a voltage mode control circuit. The PWM comparator generates a duty cycle based on these two input signals. In microcontroller based system the PWM generator is locked to this error signal.

V. DIGITAL CONTROL OF PFC

The design of a digital control system is the process of choosing the difference equation or equivalent z-domain transfer function for the controller, which will give acceptable performance for the closed loop. The performance specification can be judged from various parameters such as rise time, settling time, overshoot, closed loop frequency, bandwidth, damping ratio etc. Block diagram of a typical Digital controller is shown in Figure 2. Implementation of the controller involves solving the difference equation and interfacing ADC and DAC with the microprocessor.

A. Microcontroller based Control

In a microcontroller based application all the analog parameters and the control loops are required to be digitised. Different blocks required in Microcontroller based PFC Control is depicted in Figure 4.

As indicated in the figure three input signals are needed to implement the control algorithm. The chopper circuit is controlled by the PWM switching pulses generated by Microcontroller based on three measured feedback signals – Input voltage, Input Current and DC Bus Voltage.

B. PIC16F77 based Implementation

In the proposed scheme as shown in Figure 5, the controller is implemented using a 16F877 microcontroller.

C. PFC Software

Output from the controller is triggering pulses to IGBT to control the nominal voltage on the DC Bus. Inner Loop in the control block is current loop, whereas the outer loop in the control block forms the voltage loop.

Software flow chart of the basic PFC Controller is depicted in Figure 4. Three channels of ADC of the microcontroller are used to scan V_{ref}, V_o and I_{in} respectively

D. Proportional integral control using microcontroller

PI Controller is implemented on a micro-controller. Microcontroller is programmed to continuously scan the reference and actual feedback signal and determine the correction using PI algorithm. This correction is than converted in to ON time & OFF time by the micro-controller. Two separate counters are subsequently set in the micro-controller. Generation of pulses is done by Interrupt Driven Subroutines.

Continuous form of PI control algorithm is –

$$m(t) = K_n e(t) + K_i \int e(t) dt \quad (6)$$

Integral portion implementation in a digital controller may be written as –

$$x(t) = \int [v(t) - v_{ref}] dt + x(t_0) \quad (7)$$

Using the trapezoidal rule of integration and substituting t = KT & t_0 = (K-1).T,

$$\int (v(t) - v_{ref}) dt = \frac{T}{2} [V(KT) + V(K-1)T] - T v_{ref} \quad (8)$$

K= 1,2,..

x[(K+1)T] = T/2[V(KT)+V(K-1)T]-T.Vref + x(KT)

$m[(K+1)T] = K_p[V(KT) - V_{ref}] + K_i x[(K+1)T]$

It is assumed that the control is updated every T second. Control Signal m[(K+1)] is applied at t = (K+1)T, K=0,1,2,3,……

PI Controller thus implemented through above logic is tested and depicted in Figure 7. This output is the oscillogram recorded on Tectronix Digital Storage Oscilloscope. This was a general algorithm but this can be implemented in any application with minor adjustments. By tuning the K_P and K_I we can control different parameters such as overshoot, settling time etc.

E. Analog to Digital Conversion

Selection of suitable ADC for design of controller is also an important decision to be made. Main criterions for choosing an ADC are resolution and speed. Earlier versions of microcontrollers needed external ADC to be connected, but new microcontrollers have inbuilt ADC module. The proposed system uses

F. Pulse Width Modulation

Since most of power electronics application use PWM to convert signal into digital information, implementation of PWM on microcontroller becomes important. PWM requires use of Timers. Microntrollers like PIC have inbuilt PWM module that require only Duty Cycle and frequency information. For implementation of PWM through other microcontrollers we may use two timers one for calculation of T (1/f) and other for ON time (T1).Following logic may be followed.

Frequency of PWM pulse = f

Time period for PWM pulse T = 1/f

Duty Ratio = D

On Time T1 = DxT

Off Time T2 = T-T1

So 2 timers may be used to generate T1 and T2.

VI. SIMULATION OF THE PFC

Power factor correction scheme is simulated on the MATLAB SIMULINK as shown in figure 6. Converter parameters as chosesen are given in Table 4.

In order to maintain good EMI performance and reduced switch current rating the PFC boost converter is usually operated in continuous conduction mode (CCM). Power Circuit is a boost converter as depicted, based on IGBT. Capacitor used for bulk energy storage is located on the right side of the circuit. Firing Pulses to IGBT are generated by the proposed controller.

VII.SIMULATION AND TEST RESULTS

Figure 9 to 11 depict the results obtained from the PSIM Simulation. Figure 9 is indicative of the Input voltage and input current. Figure 7 shows the input voltage and output current of the PFC in steady state. Both are fairly stable. Figure 10 shows that output voltage. This figure shows the output voltage when the step input is applied as reference. As we can see the output voltage is regulated within 1% of the desired output voltage.

Controller is used to generate the pulses for IGBT. This is done through PWM pulses. PWM duty ratio of the pulses to IGBT is shown in figure 11.

VIII.CONCLUSIONS

Controller Design for PFC is presented in this paper. Simulation is carried out on MATLAB are reported. Further work on the implementation of PFC for application of BLDC and DC drive is going on and it is expected to be completed soon. Though the microcontroller based controller for PFC in average s mode is presented here it can be applied to other topologies with minor correction in the software.

REFERENCES

[1] Rajesh Ghosh and GNarayan," A Single Phase Boost Rectifier for wide Range of Load variation, IEEE Transaction on Power Electronics Vol.22 No.2 March 2007 pp470-479.

[2] Sakda Somkun, Panarit Sethakul, Uthen Kamnarn and Viboon Chunkag,"Simulation of DSP-based Control of Paralleled Boost PFC with Minimized Current Sensors

[3] W Zhang, G.Feng, Y-F Liu and B Wu, " A digital power factor correction (PFC) control strategy optimized for DSP," IEEE Transactions on Power Electronics vol 21 no.5 pp 1356-1363 Sept. 2006.

[4] F.V. P. Robinson and V. Chunkag, "Parallel connection of single-switch three-phase power-factor correction converters for interleaved switching," IEE Electric Power Applications, vol. 144, pp. 423-433, Nov. 1997.

[5] DRAGAN MAKSIMOVIC, ALEKSANDAR M. STANKOVIC, V. JOSEPH THOTTUVELIL, AND GEORGE C. VERGHESE, Modeling and Simulation of Power Electronic Converters" PROCEEDINGS OF THE IEEE, VOL. 89, NO. 6, JUNE 2001

[6] Milan M. Jovanovic, and Yungtaek Jang," State-of-the-Art, Single-Phase, Active Power-FactorCorrection Techniques for High-Power

Applications—An Overview" IEEE TRANSACTIONS ON INDUSTRIAL ELECTRONICS, VOL. 52, NO. 3, JUNE 2005.

[7] Dake He and R. M. Nelms," Fuzzy Logic Average Current-Mode Control for DC–DC Converters Using an Inexpensive 8-Bit Microcontroller "IEEE TRANSACTIONS ON INDUSTRY APPLICATIONS, VOL. 41, NO. 6, NOVEMBER/DECEMBER 2005

[8] Dake He and R. M. Nelms," Average Current-Mode Control for a Boost Converter Using an 8-bit Microcontroller"

[9] D. G. Lamar, A. Fernaindez, M. Arias, M. Rodriguez, J. Sebastian," A Unity Power Factor Correction Preregulator with Fast Dynamic Response Based on a Low-Cost Microcontroller"

[10] Diego G. Lamar, Arturo Fernández,,Manuel Arias,Miguel Rodríguez,, Javier Sebastián, and Marta Maria Hernando," A Unity Power Factor Correction Preregulator With Fast Dynamic Response Based on a Low-Cost Microcontroller" IEEE TRANSACTIONS ON POWER ELECTRONICS, VOL. 23, NO. 2, MARCH 2008

[11] Maksimovic D., R. Zane, and R. Erickson. 2004. Impact of digital control in power electronics. In Proceedings of the IEEE 16th International Symposium on Power Semiconductor Devices and ICs. May: 13–22.

Class	Appliances/ Equipments
Class A	Balanced 3-phase equipment household appliances excluding equipment identified as class D, tools, excluding portable tools, dimmers for incandescent lamps, audio equipment, and all other equipment, except that stated in one of the Class B, Class C or Class D equipment
Class B	Portable tools arc welding equipment which is not professional equipment
Class C	Lighting equipment
Class D	PC, PC monitors, radio, or TV receivers. Input power P <=600 W

TABLE 1- CLASSES OF EQUIPMENTS

Harmoics (n)	Class of the Equipment			
	Class A (A)	Class B (A)	Class C (% of fund)	Class D (mA/W)
Odd Harmonics				
3	2.30	3.45	30*λ	3.4
5	1.14	1.71	10	1.9
7	0.77	1.1555	7	1.0
9	0.40	0.60	5	0.5
11	0.33	0.495	3	0.35
13	0.21	0.315	3	3.85/13
15-39	0.15*15 /n	0.225*1 5/n	3	3.85/n
Even Harmonics				
2	1.08	1.62	2	-
4	0.43	0.645	-	-
6	0.30	0.45	-	-
8-40	0.23*8/ n	0.345*8 /n	-	-

TABLE-2 HARMONIC STANDARD

		2006	2007	2008	2009	2010	2011	CAGR
Embedded AC-DC		663.4	724.9	790.1	862.2	942.8	1025.4	9.1%
External AC-DC	Adapters	184.8	211.2	239.3	267.7	297.2	337.5	12.8%
	Off-line Battery Charger	1.5	1.7	1.8	2.0	2.2	2.5	10.8%
Motor Dries		221.7	238.9	257.5	278.0	300.1	324.2	7.9%
Lighting Ballasts		1013.8	1131.3	1257.3	1396.7	1553.8	1731.1	11.3%
Total		2085.2	2308	2546	2806.6	3096.1	3420.7	10.4%

Table 3 World Wide Power Supply Market (millions of units)

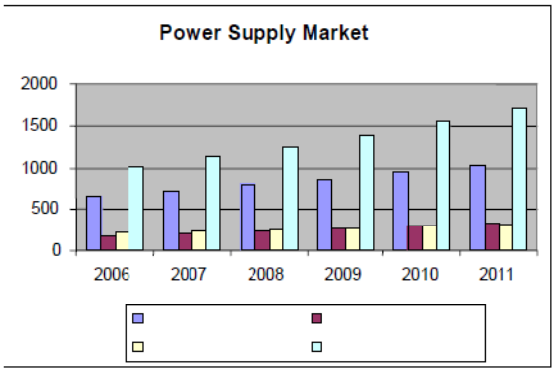

Fig. 1 : Growth of Power Supply market

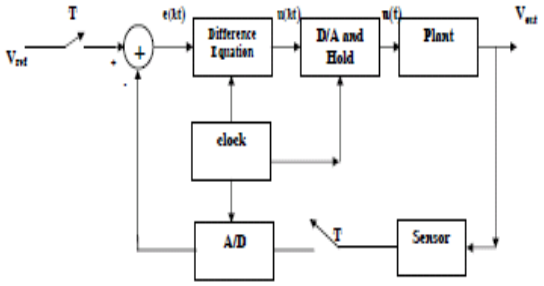

Fig. 2 : Digital Controller

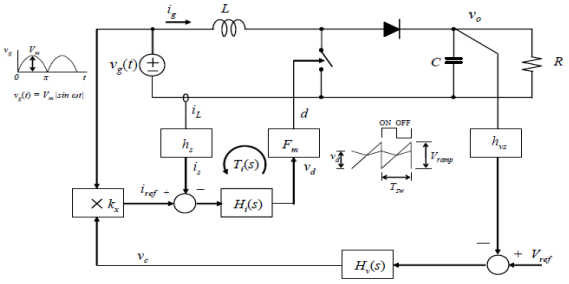

Fig. 3 : General PFC Average current mode controller

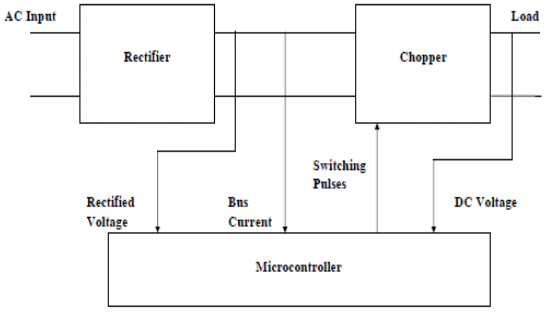

Fig. 4 : Microprocontroller based Control

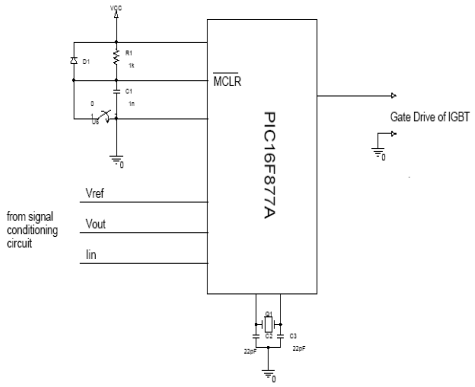

Fig. 5 : Schematic of PIC based controller

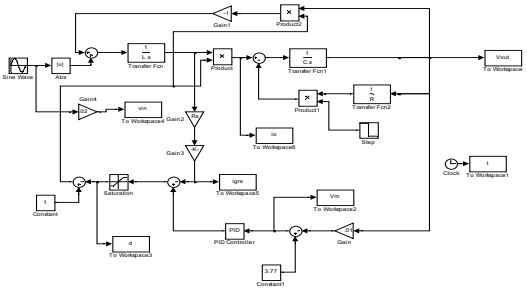

Fig. 6 : MATLAB Simulation Model

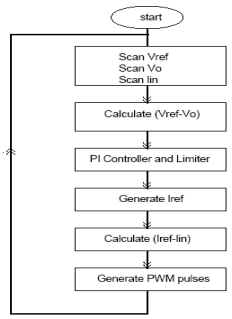

Fig. 7 : Software Flow chart

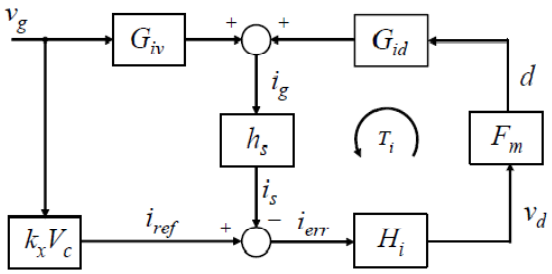

Fig. 8 : PFC Converter Transfer Functions

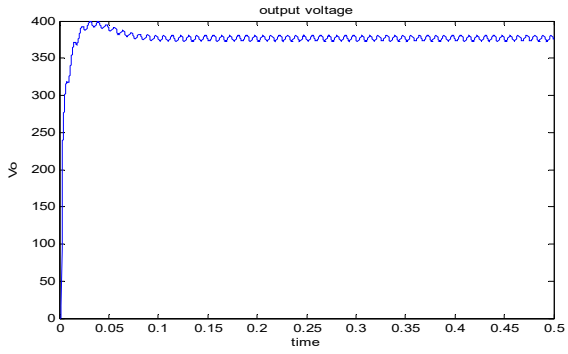

Fig. 9 : Simulated Result -Output Voltage as a result of step input

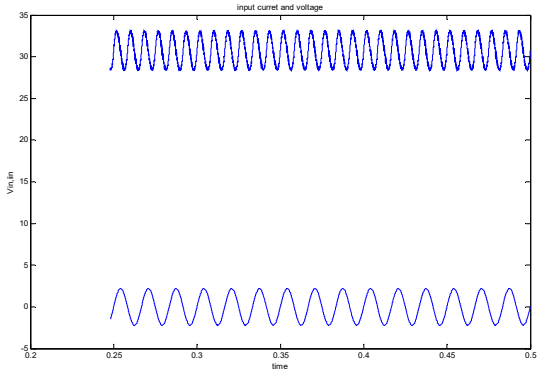

Fig. 10 : Simulated Result - Input Voltage & Current

TABLE – 2 CONVERTER PARAMETERS

Parameter	Value
V_g	200V
R	470 Ω
C	330μF
L	2.5 mH
R_s	0.1 Ω

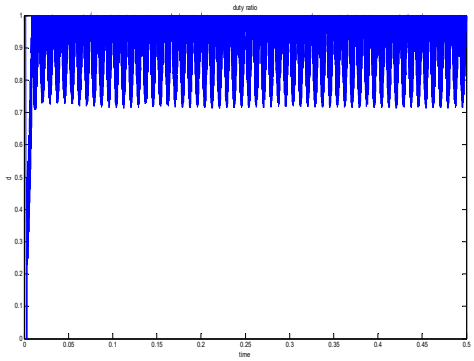

Fig. 11 : Simulated Result – Duty Raio of the Pulses

◈◈◈

Transient Analysis of EHVAC Circuit Breakers for Inductive and Capacitive Current Switching in 400kV IEEE 14bus System

Rajaramamohanarao Chennu, S Sudhakara Reddy, V S Nanda Kumar, M Chandra Sekahr & Maroti

High Power Laboratory, Central Power Research Institute, Bangalore, India

Abstract **-** The switching transients generated from switching of low inductive and capacitor current for a 400kV, IEEE 14 bus systems are presented. The simulations are carried out using the software EMTDC/PSCAD, corresponding results of transient over voltages and inrush currents for different types of capacitive and inductive current switching including shunt reactor switching, single capacitor bank switching and back to back capacitor switching etc. the results are described in detail. In this paper the testing requirements for different types of capacitive current switching and inductive current switching as per IEC international standards are also discussed.

Keywords **-** *Shunt reactor, Shunt Capacitor, switching operation, inrush currents, current chopping, Recovery and reignition, LV breakers, IEC standard.*

I. INTRODUCTION

The shunt reactors and capacitors are used to control the eactive power compensation in any electrical system. During the light load or no load the over voltages are produced by line capacitance, the shunt reactors are switched in to the system to absorb the reactive power in the system and to maintain the system voltage. Capacitor banks are designed for industrial, utility and power systems to improve power factor, increase system capacity, reduce harmonic distortion and improve voltage regulation. Since the load conditions fluctuate frequently, the shunt reactors and the capacitor banks must be switched on and off many times in a day according to the load cycle and system reactive power.

The switching of shunt reactor and capacitor will leads to transient disturbances in power systems, which may damage key equipments. The currents, which are mainly inductive in case of shunt reactors and capacitive in case of shunt capacitor banks. These currents are very small compared to nominal current of the circuit breakers, and even 200 times smaller than the short Circuit currents [1].

While switching in the circuit breakers must with stand the inrush current transients of high frequencies. When disconnecting the reactors and the capacitors form the system the circuit breaker chops the current before the current zero, which in turns generates high voltages known as the chopping overvoltages. These overvoltages can be calculated by energy balance in the switching circuits. These switching frequencies are in the range of 1 kHz to the 5 kHz [2]. In addition to the overvoltages caused by chopping, Transient recovery Voltage (TRV) also appears across the circuit breakers grading capacitance after current interruption.

The TRV depends on the source side parameters like inductance and the line capacitance etc.. These over voltages sometimes cause the restriking, which inturn generate even higher transient voltages. This phenomenon might damage the Circuit Breaker, corresponding capacitor or reactor banks. The Circuit breaker must be able to with stand these TRV and the over voltages generated by current chopping.

During the opening operations the transient recovery voltage (TRV) across the circuit breaker can rise to very high values and that can initiate breaker restrike which in turn generates even a higher overvoltage. Consequently, any re-strike implies additional stress for capacitor and circuit breaker, which reduces their lifetime or – in some extreme cases, if multiple re-strikes damages the capacitor and circuit breaker immediately. Depending on the system parameters the di/dt of high frequency current at current zero may reach greater than the current quenching capability of breaker, causing prolongation of arcing time and breaker fails to interrupt the fault current.

This paper discusses the transients generated by interrupting low inductive and capacitor current switching for a 400kV IEEE14 bus system shown in fig.1. The simulations are carried out using the software

EMTDC/PSCAD, corresponding results of transient over voltages for different types of capacitive and inductive current switching single capacitor bank switching and back to back capacitor switching etc. the details results are described in detail. The testing requirements for different types of capacitive current switching and inductive current switching as per international standards are also discussed.

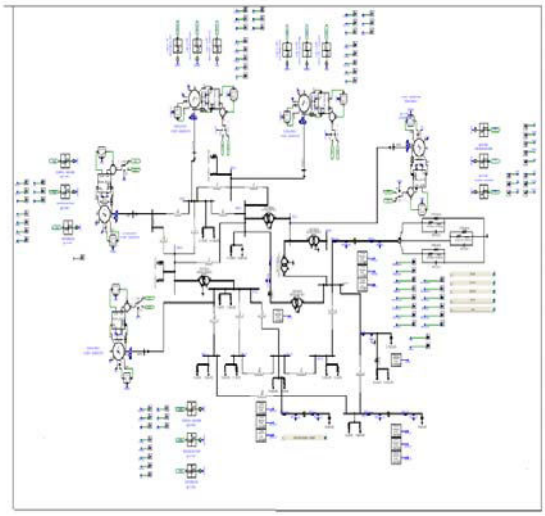

Fig. 1 : IEEE14 bus transmission system

II. CAPACITOR BANK SWITCHING

Depending on the type of capacitor switching transients are classified in to five types [2] 1) Single bank energization inrush, 2) back-to-back energization, 3) out rush into a nearby fault, 4) voltage magnification, and 5) transient recovery voltage (TRV).

In case of single bank energization switching only one capacitor is connected to the grid. The inrush current is mainly affected by the inductances on the path from the source to the capacitor [3]. The inrush current in to the capacitor may be approximated as [3].

$$i(t) = \frac{V(0)}{Z_0} sinw_0 t \qquad (1)$$

Where $Z_0 = \sqrt{\frac{L}{C}}$, $w_0 = \frac{1}{\sqrt{LC}}$

L= Line inductance

C= Value of capacitor

V(0) is the difference between the source voltage and the initial voltage of capacitor at the instant of energization.

Z_0= is total system characteristic impedance at the instant of energization.

The energization inrush currents when switching a 25MVAR capacitor bank to IEEE14 bus system is shown in fig.2a and fig.2b. In fig.2a the capacitor bank is switched in at maximum value of phase voltage and switched at zero of the phase voltage is showed in fig.2b.

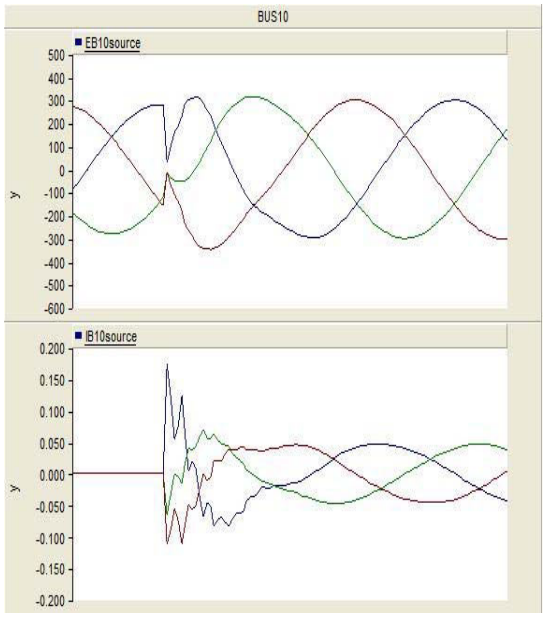

Fig. 2a : Single capacitor bank energization

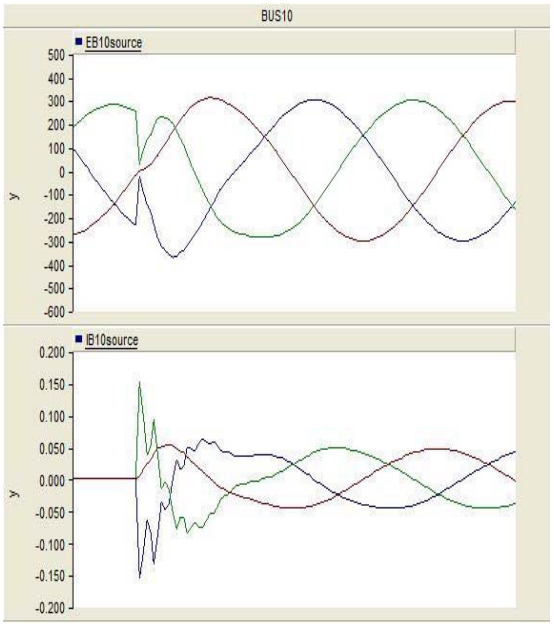

Fig. 2b : Single capacitor bank energization

From fig.2a & fig.2b it is clear that transient inrush current are minimum when switching the capacitor bank

at phase voltage zero and maximum when switched at peak value of phase voltage.

In case of back to back switching, where one capacitor (C_1) is already connected to the grid, and another capacitor bank (C_2) one is connected afterwards, the inrush currents are mainly influenced by the inductances (L_B) in the path from the first to the second capacitor. The expression for the high frequency transient current riding on steady state is given by [3]. The inrush current is shown in fig.3.

$$i(t) = \frac{V(0)}{Z_0} sinw_0 t \qquad (2)$$

Where $Z_0 = \sqrt{\frac{L_B}{C_{eq}}}$, $w_0 = \frac{1}{\sqrt{L_B C_{eq}}}$ & $C_{eq} = \frac{C_1 C_2}{C_1 + C_2}$

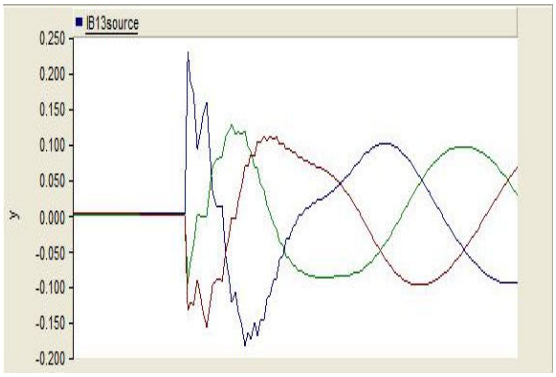

Fig. 3 : Back to back capacitor bank energization

The change in peak value of transient inrush current with switching angle is presented in fig.4. The peak value of transient inrush current is varied from 3.7pu to 3pu.

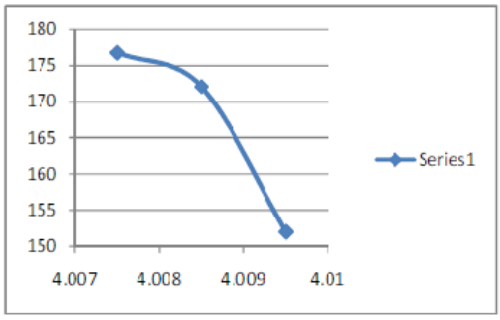

Fig. 4 : Transient inrush current Vs switching time.

III. SHUNT REACTOR SWITCHING

The simulation is carried out in PSCAD on 400kV, IEEE14 bus system which is showed in fig. 1.

The shunt reactor used for simulation purpose is wye connected with the neutral solidly grounded, showed in fig.5.

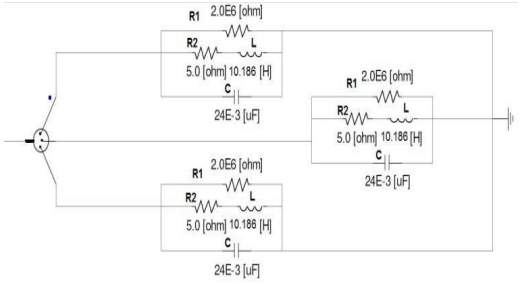

Fig. 5 : The shunt reactor

The parameters for the 50 Mvar shunt reactor are R1=2MΩ, R2=5Ω, L=10.196H and C=2.4nF.

When the shunt reactor is energized by circuit breaker very high inrush currents with long time constant occurred [4], which is presented in fig.6. In fig.6 first oscillogram is source voltage and second id inrush current and third is the voltage at reactor terminal. The small transient current in the order of 10kHz [4] depends on the system parameters is also observed. The transient over voltages at the time of switching are also presented.

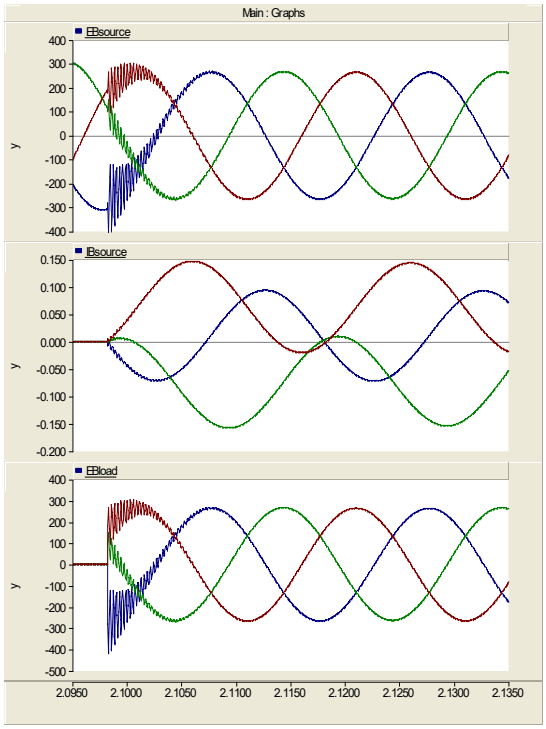

Fig. 6 : Shunt reactor energisation transients

From fig.6 and 7 it is clear that the transient overvoltages depend on the instant of reactor energization. There are no transient overvoltages when the reactor is energized at zero crossing of phase voltage and the transient over voltages are maximum when the reactor is energized at peak value of phase voltage.

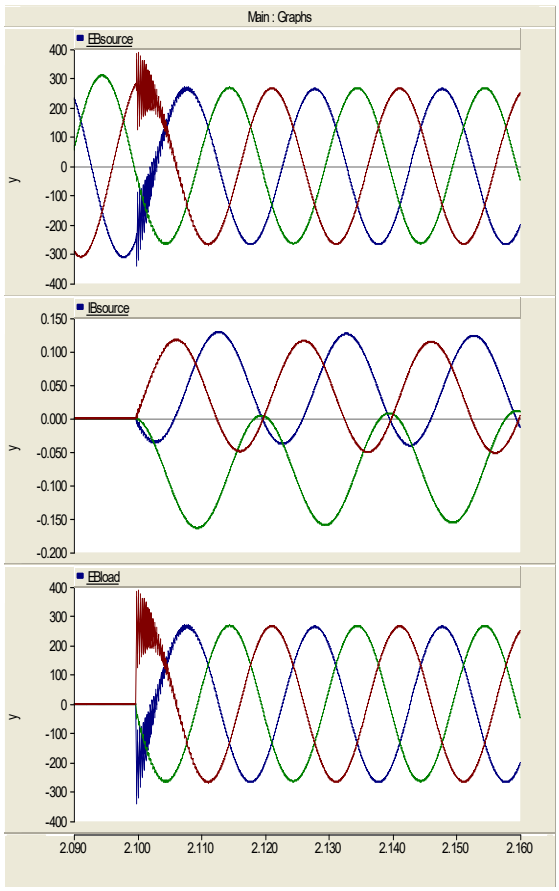

Fig. 7 : Shunt reactor energisation transients

When de energizing the shunt reactor the current interrupted by the breaker is very small compared to rated breaking capacities. The medium used for arc extinguishing will develop fast residual column resistance and abrupt current interruption before its natural current zero crossing may occur [5,6]. This phenomenon is called current chopping. The stored energy released by the reactor will cause electromagnetic transients that lead to switching overvoltages. These transients depend on the system configuration and its parameters.

Fig. 8 shows the transient phenomena developed by interrupting the shunt reactor and the current chopping phenomena.

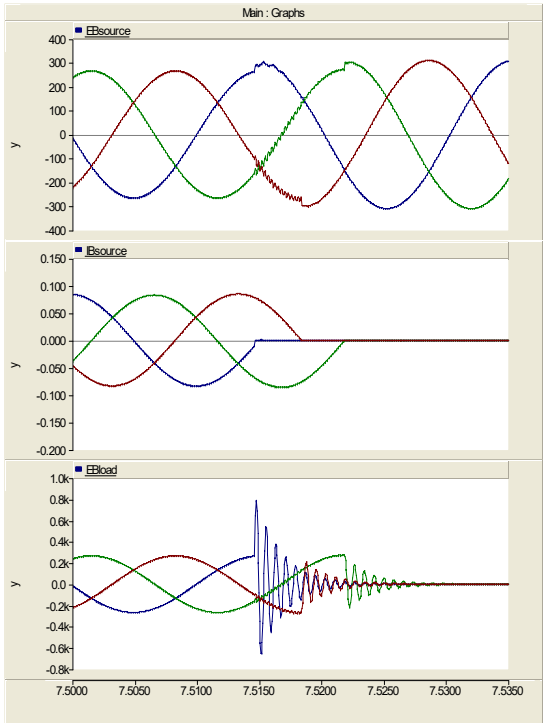

Fig. 8 : Shunt reactor de-energisation transients

The over voltages generated on the reactor terminals depends on the value of chopping current. Fig. 9 presents the variation of the over voltages with the chopping current. The chopping voltages can sometimes 20-30pu based on the chopping current. The switching over voltages generated by current chopping should not exceed 80% of the peak value of the switching impulse with stand voltage [7]. Without reignition the over voltages never exceed the switching over voltages [1].

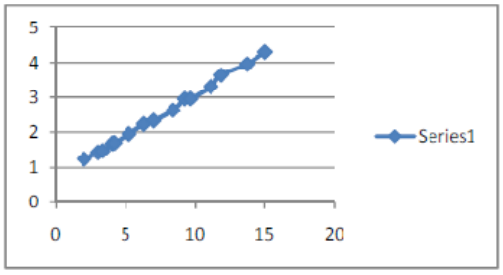

Fig. 9 : Chopping overvoltages Vs chopping currents.

The over voltages generated is the because of the inter phase coupling between inductance and the capacitance. By varying the capacitance by damping the can be changed. Fig.10 shows the damping of chopping over voltages on reactor terminal side by increasing C by ten times.

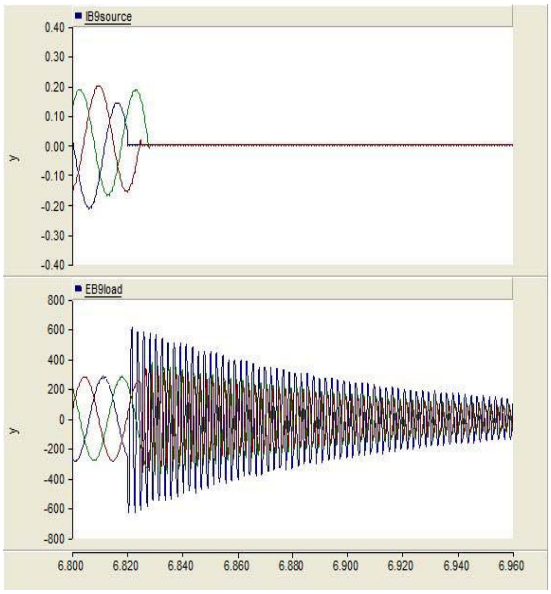

Fig. 10 : Chopping overvoltages with increased C.

IV. SHUNT REACTOR SWITCHING AS PER IEC

Reactor switching is an operation where small difference in circuit parameters can produce large difference in the severity of the duty. Shunt reactor current switching tests are applicable to 3-phase A.C. circuit breakers having rated voltages of 12kV and above. The switching tests can be either field tests or laboratory tests. For laboratory tests, the standard circuits are specified in order to demonstrate the ability of the circuit breaker to interrupt reactor currents and to determine chopping characteristics and re-ignition behavior. For laboratory tests, standard circuits are specified for three-phase and single-phase shown in fig.3 and fig.4 of IEC 61233. In the Characteristics of the supply circuit, the source impedance shall not be smaller than that corresponding to the rated short circuit current of the circuit breaker, nor larger than 10% of the inductance of the load circuit, and the source capacitance shall be at least 10 times the load capacitance. The TRV of the supply circuit has a negligible influence on that of the complete circuit and is therefore not specified. In Characteristics of the load circuits, the load circuits shall consist of a reactor or alternatively, an air-cored or iron-cored reactance with appropriate shunt capacitance and resistance so as to produce a prospective transient voltage not less severe than the values specified in table 2 of IEC 61233. For shunt reactor switching test, the reactance of the 3-phase and 1-phase load circuit shall be adjusted to give the breaking currents as per IEC 61233 clause of 4.61 and 4.6.2 respectively.

The earthing of the test circuit, for circuit breakers with rated voltages below 245kV, the load of the three-phase test circuit shall be unearthed, while the neutral point of the supply is earthed and for circuit breakers rated 245 kV and above, both the supply and the load of the three-phase test circuit shall be earthed.

For three phase tests, the test voltage measured between the phases at the circuit breaker location immediately prior to opening shall, as near as possible, be equal to the rated voltage U of the circuit breaker. For single phase laboratory test, the test voltage measured at the circuit breaker location immediately before the opening shall, as nearly as possible, be equal to the product of U/√3 and factor of 1.0 for full pole tests of circuit breaker rated 245 kV and above, 1.5 for full pole tests of circuit breaker rated 170 kV and below.

The reactor switching test duties shall consist of two three-phase test series or three single phase test series using the supply circuit detailed in Table 3 of IEC 61233. Inorder to analyse the concept of reactor switching test, supply side voltage (phase to earth), voltage across circuit breaker terminals, load side voltage(phase to earth) at the terminal of the load reactor, load side neutral point voltage to earth (in three phase tests), current though the circuit breaker quantities should be recorded by oscillograph or 0ther suitable recording techniques with bandwidth and time resolution high enough. The circuit breaker shall have successfully passed the tests if the current is successfully interrupted.

V. CAPACITOR SWITCHING AS PER IEC

Capacitance switching applications involve not only interrupting capacitive currents, but also the energizing of overhead lines, cables and capacitor banks. These tests are applicable to all circuit-breakers to which one or more of rated line-charging breaking current, rated cable-charging breaking current, rated single-capacitor bank breaking current, rated back-to-back capacitor bank breaking current, rated single capacitor bank inrush making current, rated back-to-back capacitor bank inrush making current ratings have been assigned.

Re-ignitions during the capacitive current switching tests are permitted. According to their restrike performances circuit breakers are categorized into two classes: class C1: low probability of restrike during capacitive current breaking as demonstrated by specific type tests (clause 6.111.9.2 of IEC 62271-100); class C2: very low probability of restrike during capacitive current breaking as demonstrated by specific type tests (clause 6.111.9.1 of IEC 62271-100).

In laboratory tests the lines and cables may be partly or fully replaced by artificial circuits with lumped

elements of capacitors, reactors or resistors. When capacitors are used to simulate overhead lines or cables, a non-inductive resistor of a maximum value of 5% of the capacitive impedance inserted in series with the capacitors. Higher values may unduly influence the recovery voltage. If with this resistor connected, the peak inrush current is still unacceptably high, then an alternative impedance (RL combination) used instead of the resistor, provided that the current and voltage conditions at the instant of breaking and the recovery voltage d o not differ significantly from the specified values.

For direct three-phase laboratory tests, the test voltage measured at the circuit breaker location immediately before the opening shall be not less than the rated voltage Ur of the circuit breaker. For direct single-phase laboratory tests, the test voltage measured at the circuit breaker location immediately before the opening shall be not less than the product of Ur/√3 and the product of capacitive voltage factor Kc as per clause 6.111.7 of IEC 62271-100. The test currents for various test-duties are defined as per clause 6.111.9 of IEC 62271-100. Preferred values of rated capacitive switching currents are given in table 9 of IEC 62271-100.

Capacitive current switching tests for class C2 circuit breakers shall be made after performing test-duty T60 as a preconditioning test. For circuit breakers rated less than 52 kV, the manufacturer may choose to add other test-duties to the T60 preconditioning tests. The capacitive current switching tests for class C2 circuit breaker shall consist of the test-duties as specified in table 30 of IEC 62271-100. The preferred order for the line-charging or cable-charging current switching tests is terminal fault T60 (mandatory at the beginning), capacitive current switching (test-duty 1) and capacitive current switching (test-duty 2). The mandatory order for the capacitor bank current switching tests is terminal fault T60 (mandatory at the beginning), capacitive current switching (test-duty 2) and capacitive current switching (test-duty 1). In each test-duty, the order of the operations performed from clause 6.111.9.1.2 to 6.111.9.1.5 of IEC 62271-100.

Capacitive current switching tests for class C1 circuit breakers shall consists of test duties as specified in table 31 of IEC 62271-100 without preconditioning. The behavior of circuit breaker during making and breaking tests, the circuit breaker shall not 1) show signs of distress, 2) show harmful interaction between poles and to earth, 3) show harmful interaction with adjacent laboratory equipment, 4) exhibit behavior which could endanger an operator.

The criteria to pass the test for class C1, the circuit breaker shall have successfully passed the tests if up to one restrike occurred during test-duties1 and 2. If two restrike occurred during the complete test-duties 1 and 2, then both test-duties shall be repeated on the same apparatus without any maintenance. If no more than one additional restrike happens during this extended series of tests, the circuit breaker shall have successfully passed the test. External flashover and phase-to-ground flashover shall not take place.

The criteria to pass the test for class C2, the circuit breaker shall have successfully passed the tests if no restrike occurred during test-duties1 and 2. If one restrike occurred during the complete test-duties 1 and 2, then both test-duties shall be repeated on the same apparatus without any maintenance. If no additional restrike happens during this extended series of tests, the circuit breaker shall have successfully passed the test. External flashover and phase-to-ground flashover shall not take place.

VI. CONCLUSION

The shunt reactor and capacitor bank switching is frequent, which causes the transient over voltages and inrush currents. The over voltages can damage the insulation of the switching load or the power system equipment or the breaker it self.

An IEEE14 bus 400kV system is simulated for both shunt reactor and capacitor bank energisation.

- ◊ The switching transient over voltages at the time energisation of shunt reactor or capacitor depends on the instant of energistion.
- ◊ The damping of the chopping over voltages depends on the interphase capacitance of the shunt reactor.

The testing of shunt reactor and capacitor as per IEC standard is presented.

REFERENCES

[1] Ivo Uglešić, Sandra Hutter, Miroslav Krepela, Božidar Filipović- Grčić and Franc Jakl " "Transients Due to Switching of 400 kV Shunt Reactor" presented at International Conference on Power Systems Transients, Río de Janeiro, Brazil, June 24-28, 2001.

[2] H.Abdul Hamid, N.Harid and A.Haddad "Determination of Transient Overvoltages during Shunt Reactor Deenergization", IEEE Universities Power Engineering Conference (UPEC), 2009 Proceedings of the 44th International, 978-1-4244-6823-2, pp.1-4, 2009.

[3] Govind Gopakumar, Huihua Yan, Dr. Bruce A. Mork Kalyan K. Mustaphi, "SHUNT

CAPACITOR BANK SWITCHING TRANSIENTS: A TUTORIAL AND CASE STUDY," Vol 2 2002.

[4] Ariel Rivera-Colón, Juan L. Vargas-Figueroa and Lionel R. Orama-" Transient Analysis of Shunt Reactor Switching (December 2005)" final project of INEL 6077, 2005.

[5] G. W. Chang, H. M. Huang, J.H. Lai, "Modeling SF6 Circuit Breaker for Shunt Reactor Switching Transient Analysis," presented at POWERCON 2004, Singapore, 21-24 November 2004.

[6] I. Uglesic, S. Hutter, M. Krepela, B. Filipovic, F. Jakl "Transients Due to Switching of 400 kV Shunt Reactor" presented at International Conference on Power Systems. Transients, Río de Janeiro, Brazil, June 24-28, 2001.

[7] IEC1233 - Technical Report Type 2: "High-Voltage Alternating Current Circuit-Breaker-Inductive Load Switching", First Edition, 1994.

[8] IEC62271-100High-voltage switchgear and controlgear – Part 100: High-voltage alternating-current circuit-breakers, Ed-2, 2010.

◈◈◈

Overview of Honeypot Security System for E-Banking

Prajakta Shirbhate, Vaishnavi Dhamankar, Aarti Kshirsagar, Purva Deshpande & Smita Kapse

Department of Computer Technology, YCCE, Nagpur, Maharashtra, India

Abstract **-** This paper presents a proactive defense scheme based on Honeypot security system (HPSS). We propose an improved approach based on Intruder Detector System (IDS) which enhances the security of cyber. HPSS provide improved attack prevention, detection and reaction information, drawn from the log files and other information captured in the process. Honeypot security system can be best defined as follows:

"A honeypot is a security resource whose value lies in being probed, attacked or compromised.[1] However, the electronic banking system users still face the security risks with unauthorized access into their banking accounts by non-secure electronic transaction hence it need to build reliable system which holds the identity of both the sender and the receiver."

Keywords - *Honeypot security system, Intrusion detection system, Firewall protection, Security for banking services, Decoy system.*

I. INTRODUCTION

Honeypot is an exciting new technology with enormous potential for the security community. It is resource which is intended to be attacked and compromised to gain more information about the attacker and his attack techniques [3]. The most of the attacks by a hacker would like to attack on the database concerning the username, the password and their respective account numbers. After acquisition of the same the hackers would very conveniently trespass the security walls of authentication and authorization and thereby making the transaction official [2].

Honey Pots are fake computer systems, setup as a "decoy", that are used to collect data on intruders. A Honey Pot, loaded with fake information, appears to the hacker to be a legitimate machine. While it appears vulnerable to attack, it actually prevents access to valuable data, administrative controls and other computers. Deception defenses can add an unrecognizable layer of protection. As long as the hacker is not scared away, system administrators can now collect data on the identity, access, and compromise methods used by the intruder. The Honey Pot must mimic real systems or the intruder will quickly discover the 'decoy'. Honey Pots are set up to monitor the intruder without risk to production systems or data. If the Honey Pot works as intended, how the intruder probes and exploits the system can now be assessed without detection. The concept of a Honey Pot is to learn from the intruder's actions. This knowledge can now be used to prevent attacks on the "real", or production systems, as well as diverting the resources of the attacker to a the 'decoy' system.[3][4]

The remaining of this paper is organized as follows. Section 2 provides related work, section 3 provides Review on Honeypot security system and section 4 provides conclusion.

II. RELATED WORK

Many different approaches to building detection models have been proposed. A survey and comparison of detection techniques is given in this paper presents an approach for modeling normal sequences using look ahead pairs and contiguous sequences. This paper presents a statistical method to determine sequences which occur more frequently in intrusion data as opposed to normal data. This paper uses neural networks to model normal data and examines unlabeled data for anomaly detection by looking at user profiles and comparing the activity during an intrusion to the activity under normal use [1].

The paper shows following a point which summarizes some key events [5].

In 1997 - Version 0.1 of Fred Cohen's Deception Toolkit was released, one of the first honeypot solutions available to the security community.

In 1999 - Formation of the Honeynet Project and publication of the "Know Your Enemy" series of papers. This work helped increase awareness and validate the value of honeypots and honeypot technologies.

In 2000/2001 - Use of honeypots to capture and study worm activity. More organizations adopting honeypots for both detecting attacks and for researching new threats.

In 2002 - a honeypot is used to detect and capture in the wild a new and unknown attack.

This paper proposes that any security system can be made more reliable and effective using Honeypot security system because it not only prevent the person illegally accessing accounts but detect him. It also shows the list of attacks and counts the no. of appearances [2]. Same concept is introduced in paper but more it tells that the attack is being done on the dummy database remaining true database unaffected [3].

Some research states that it can be used in military field to detect unknown codes[7] while other paper suggest it can be used in banks and various financial company[10].

III. REVIEW ON HONEYPOT SECURITY SYSTEM

Traditionally, honeypots have been used to detect or capture the activity of outsider or perimeter threats. The purpose of these honeypots varied. Some organizations are interested in learning what threats exist and gaining intelligence on those threats, others want to detect attacks against their perimeter, while others were attempting early warning and prediction of new attack tools, exploits, or malicious code.

A. *Intrusion Detection Honeypot Security System (IDHPSS)*

False positives are a constant challenge for most organizations. But a honey pot is a host that captures unauthorized activity.

The honey pot reduces false negatives by capturing absolutely everything that enters and leaves itself. This means all the activity that is captured is most likely suspect. As to unknown activity, even if Intruder Detection system (IDS) misses it, we have captured the activity. We can review all of the captured activity and identify the attack.

The Architecture of the Intruder Detection Honeypot Security System (IDHPSS) is shown in Figure 1. This figure shows eight essential components of the architecture: “Remote Log Server”, “Sniffer Server”, “Honey Pot”, “IDS”, “WWW Server”, Switch, Router and Fire Wall. “IDS” is the host for intrusion detection and “WWW Server” is the secured host in the network. Switch is used for the Data Control and Router for the Route Control. Another function to set up the Router is to create a network environment that is more realistically mirrors a production network. So the trap of the honey pot is not easy to be found. Traditional IDS is purely defensive. But in IDHPSS, there is enough information about threats that exist. New tools and attack patterns can be discovered. Hence, future compromise can be predicted.

1) *Architecture*

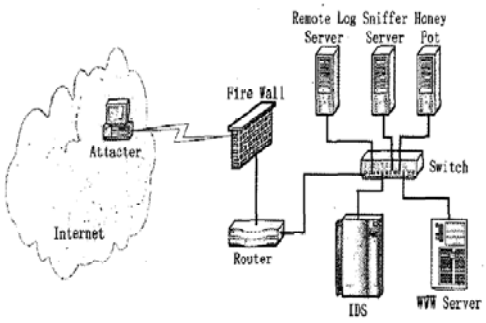

Fig. 1: Architecture of IDHPSS

The honey pot system can cooperate with Fire Wall. The system will refuse the visit of the intruder whose IP address is set in the Fire Wall as blacklist by the honey pot.

By combining data from multiple systems, the attack of the system can be predicted and attacker is sent to Honeypot for further processing.

2) Characteristics in the IDHPSS

The main characteristics that will be achieved in the AAIDHP are flexibility, configurability and security.

- *Flexibility* - Honey pot creates a network environment that more realistically mirrors a production network.
- *Configurability* - IP trap, Data Control and Route Control can be deployed dynamically.
- *Security* - Intruders can be trapped in the honey pot before an attack is made on real assets.

It is obvious that AAIDHP solves the information overload, unknown attacks, false positives and false negatives.

B. *Honeypot security system for E-Banking*

Often most users have a lack of precise information dealing with attacks on the Internet. In most cases, we just see the *results* of attacks against networks *or* specific computers. We do not have precise quantitative predications of attacks against computer systems and the tools, tactics, and motives involved in computer and network attacks are often not known in detail. Following flowchart shows how system will work according study of proposed system.

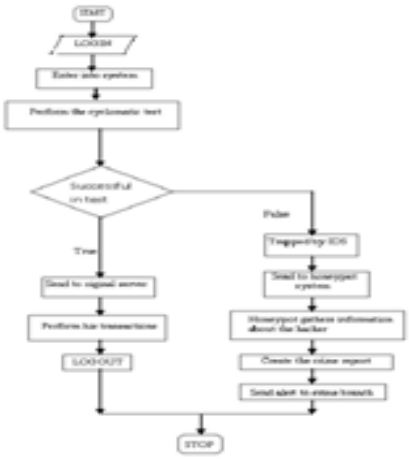

Fig. 2: Flowchart of Honeypot security system

Honeypot system secures data and data transmission from being hacked. This system represents fake version of original system. General security system provides denial of services but Honeypot security system allows hackers to enter into fake system which is this honeypot system and gathers the information of the intruder.

There are three layers to gather the information of intruder which includes:

1) IP address tracing:

This step includes the IP address tracing. Once person logins into the system first of all IP address is noted down.

In this, both the IP tracing as well as Login test is performed. If he fails to login for couple of times he will be entered into the fake system. In security systems which are present currently there will be denial of service if a person fails to login for defined iterations.

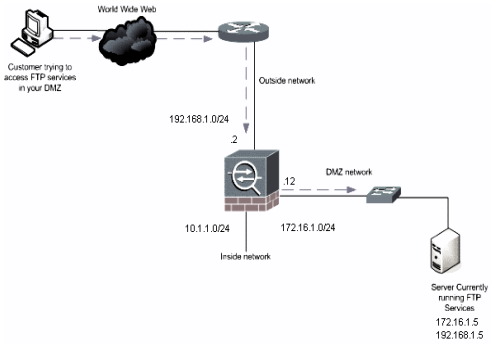

Fig. 3 : IP addressing

2) Psychometric test:

This test is performed to detect that is the person a regular and real customer or a hacker hacking other person's account.

There will be some set of questions which will be asked to the person. The answers to the questions will be known to the actual user only. If the person fails to answer the questions more than two times then he will be transferred into the fake system.

3) Captcha image:

Captcha image is used to check whether the logged person is a person or machine.

Many times it is possible that a person can use software to perform iterations and will get the password. If the password is 6 letters long then there will be 6 loops and by the combination he can get the password.

Hence captcha image phase is used to avoid this type thread. Captcha looks like following:

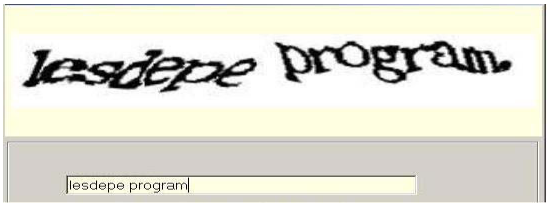

Fig. 4 : Captcha image.

Honeypot security system (HPSS) keep the records of action performed by intruder i.e. which data he is downloading, sites he is visiting. All the interactions and transmissions will be fake but he will think it is taking place actually. Hence, he will be trapped by the system and we will get the information to perform necessary action. By gathering all information about hacker HPSS will make crime report and will send it to the crime branch to perform specific actions according to his crime.

C. *Advantages Of Honey pots*

1) Small Data Sets: Honey pots only collect data while interacting with them. Many organizations logging thousands of alerts a day may log a hundred alerts with honey pots. This makes the data honey pots collect much higher value, easier to manage and simpler to analyze.

2) Reduced False Positives: One of the greatest challenges is the generation of false positives or false alerts. The larger the probability that a security technology produces a false positive the less likely the technology will be deployed. Honey pot security system reduces false positives.

3) Catching False Negatives: Another challenge of traditional technologies is failing to detect unknown attacks. The traditional computer security technologies rely upon known upon statistical detection which also suffers from probabilistic failures. Honey pots on the other hand can easily identify and capture new attacks against them. Any activity with the honeypot is an anomaly, making new or unseen attacks easily standout.

4) Encryption: It does not matter if an attack or malicious activity is encrypted, the honeypot will capture the activity. Honey pots can do this because the encrypted probes and attacks interact with the honeypot as an end point, where the activity is decrypted by the honeypot.

5) Highly Flexible: Honey pots are extremely adaptable, with the ability to be used in a variety of environments, everything from a Social Security Number embedded into a database, to an entire network of computers designed to be broken into.

6) Minimal Resources: Honey pots require minimal resources, even on the largest of networks.

7) Resources: Network Intrusion Detection Devices may not be able to keep up with network activity, dropping packets, and potentially attacks while centralized log servers may not be able to collect all the system events. Honeypots do not have this problem; they only capture that which comes to them [3].

8) Lossless: The Honeypot system creates the environment to attract the intruder and all the transactions and processing done on the system is fake. Hence it does not make any loss to accounts or data which is being hacked [2].

IV. OUTPUT

Until now we have discussed about how honeypot security system works. Following snapshot shows actual implementation of this system developed by us. This snapshot shows three layers of test that we are performing i.e. login, psychometric and capcha image. Also while login IP address is traced as shown.

Fig. : Home page

Fig : Login test

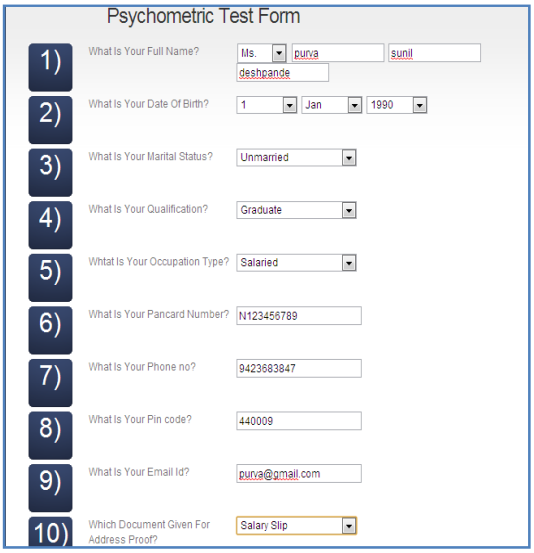

Fig. : Psychometric test

Fig. : Capcha image test

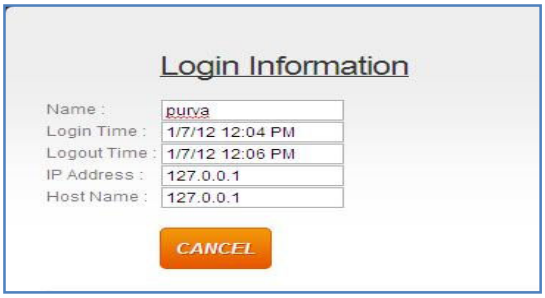

Fig. : IP tracing

After performing these tests user, if he is hacker, will be transferred to fake system and if he is real user, he will be transferred to real banking system.

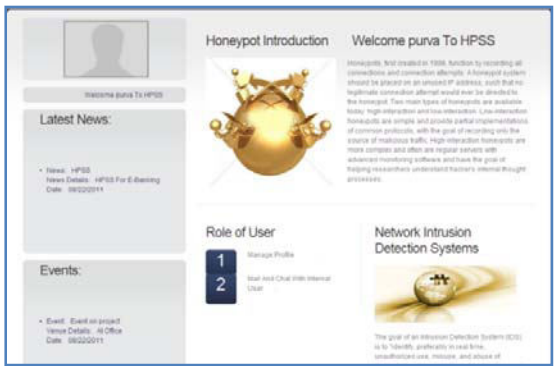

Fig. : Users account

V. CONCLUSION

Network security is a matter of social stability and national security. Honeypots are clearly a useful tool for luring and trapping attackers, capturing information and generating alerts when someone is interacting with them. The activities of attackers provide valuable information for analyzing their attacking techniques and methods. The honey pot system can cooperate with Fire Wall. The system will refuse the visit of the intruder whose IP address is set in the Fire Wall as blacklist by the honeypot. According to the destroy degree, the term of refusing the malicious visit can be short-term or long-term. By combining data from multiple systems, these data can be used for such things as early warning and prediction, statistical analysis, or identification of new tools or trends.

In future Honeypot security system can be used in various banks for their online procedures such as E-banking. It can be used for scientific or government purposes where confidential data is to be remained confidential

REFERENCES

[1] Zhi-hong Tian,Bin-xing Fang, “An Architecture For Intrusion Detection Using Honeypot”, Second international conference on machine learning and cybernetics 2003.

[2] Christian Doring,” Improving network security with honeypot.”

[3] Lanz Spitzner, “Know Your Enemy: Learning with User-Mode Linux Building Virutal Honeynets using UML”

[4] Lanz Spitzner, “Know Your Enemy: GenII Honeynets,”.http://www.honeynet.org,May, 2005.

[5] Lanz Spitzner, “Know Your Enemy: Honeywall CDROM Roo 3rd Generation Technology”, 2005.

[6] Jungsuk SONG-Kyoto University, Hiroki TAKAKURA-Kyoto University, Yasuo OKABE-Kyoto University, Cooperation of Intelligent Honeypots to Detect Unknown Malicious Codes, IEEE, 2008 .

[7] The Government of the Hong Kong Special Administrative Region, “Honeypot security” February 2008.

[8] http://www.seminarprojects.com/Thread-honeypots-seminar-report#ixzz1YOSPf8Ka Cormac Herley and Dinei Florencio, “Protecting Financial Institutions from Brute-Force Attack.

◈◈◈

Modeling of Green Energy Sources –A Solar and Wind Hybrid Model

Diksha Khare[1] & SF.Lanjewar[2]

[1]Electronics & Telecommunication Deptt., Guru Nanak Institute of Engineering and Management, Nagpur, India
[2]Electrical Engineering Deptt, G.H.Raisoni College of Engineering, Nagpur, India

Abstract **-** In parallel to developing technology, demand for more energy makes us seek new energy sources. The most important application field of this search is renewable energy resources.Wind and solar energy have been popular ones owing to abundant, ease of availability and convertibility to the electric energy. We will focus on Modeling the design and verification process for Renewable and Green Energy sources.Samples like solar,wind and tidal energy are used for making model.The term Green energy can be associated with environment-friendly Generation,transport,storage and control of electrical energy .Solar power,wind power and the natural flow of water are resources that comply with our definition of Green Energy.Since the natural fossil energy resources are limited on this planet,we have to put our focus on green power generation like solar and wind power.

Keywords **-** *component:Green Energy sources, Renewable .*

I. INTRODUCTION

The electricity sector in India supplies the world's 6th largest energy consumer.

Contribution of various power sources to generation of Electricity is :

Power plant	Electricity Generated
Thermal	67.75%
Hydroelectric	21.73%
Nuclear	2.78%
Renewable Energy sources	10.73%

Solar power

In 2010,India's installed wind generated electric capacity was 13,064 MW.In July 2009,India unveiled a $ 19 billion plan to produce 20,000 MW of solar power by 2022.With the technological developments,products which run on nonconventional energy sources will be more popular near future with proper design and materialistic advancements.

India is densely populated and has high solar insolation,an ideal combination for using solar power in India.

Solar panel : A solar cell (also called photo voltaic cell) is a device that converts the energy of sunlight directly into electricity by the photo voltaic effect.Assemblies of cells are used to make solar modules also known as solar panels.

Photovoltaic cell : A photovoltaic cell is the basic device that converts solar radiation into electricity.It consists of a very thick n-type crystal covered by a thin n-type layer exposed to the sunlight.

Cells are arranged in a frame to form a module.Modules put together form a panel.Panels form an array.Each PV cell is rated for 0.5- 0.7 v and a current of 30 mA/sq.cm.

Photovoltaic panels

Photovoltaic panels consist of several modules; modules are composed of cells which are in series. Photovoltaic cells transform luminous energy (solar) into electrical energy.

The equivalent circuit of a photovoltaic cell is shown in fig. 1.

It consists of an ideal source producing a current IPh, proportional to incident light, in parallel with a diode D. Shunt resistance Rp models the effect of leak current but in many cases this can be neglected due to its relative large value.

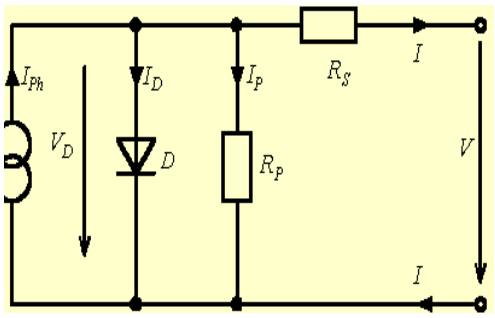

Fig. 1: PV cell model

The traditional solar panel which is fixed on a constant base is shown in fig.

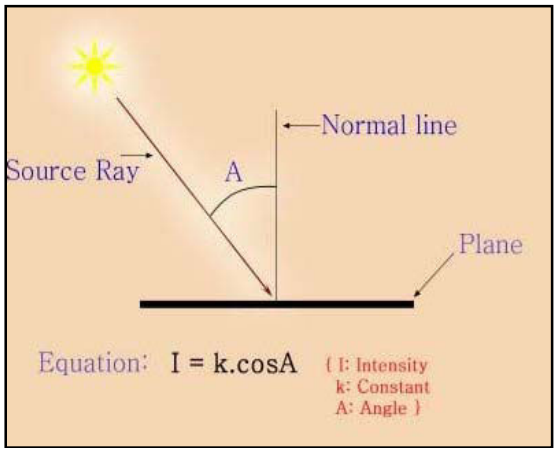

Fig. 2

The output of solar cells depends on the intensity of sunlight and the angle of incidence. The angle of incidence is the angle between the normal and an incident (that is, an incoming) light ray shown in fig. above

Wind Power

Wind Power is very popular nowadays, because of the high power that can be achieved in a efficient way.

The Wind is identified as a key natural energy resource, which contributes to reducing undesirable emissions due to fossil fuel power plant operation. Worldwide installed wind power capacity has reached 120GW at the end of 2008 with a 36% increase in comparison to the previous year. However,with the increase of wind power penetration, the technical and operational challenges associated with wind energy have also become more apparent. These challenges include, the elimination of power fluctuations, improving power quality, connection of wind farms to weak grids, prediction of wind power and changes in operating strategies of conventional power plants .Irregular variations of the wind power are the root cause of the first challenge, and more or less partial cause of the others.

Wind turbines are used to convert the wind power into electric power.Electric generator inside the turbine converts the mechanical power into the electric power. Wind turbine systems are available ranging from 50w to 2-3 MW.

Mechanical output of turbine of wind generator is dependent on the speed of turbine.For small turbines,wind speed is about 3.5m/s.Large wind power plants require wind speed of 6m/s.but wind speeds higher than this are available in many locations.

Hybrid Electric systems

Hybrid Electric systems combines wind and solar photovoltaic technologies offering several advantages over either single system.

Wind speeds are low in summer when the sun shines the brightest and longest.The wind is strong in winter when less sunlight is available.Because the peak operating times for wind and solar systems occur at different times a day and year,hybrid systems are likely to produce power when required.

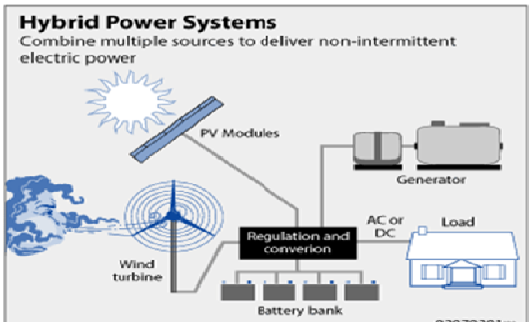

Fig. 3 : Hyrid power system solar and wind.

The hybrid unit contains two complete generating plants,a solar plant and a wind system.The two sources are connected in parallel,the power is connected to a DC to AC inverter and is then supplied from the inverters output to a single phase load.

Simulation model for wind generator

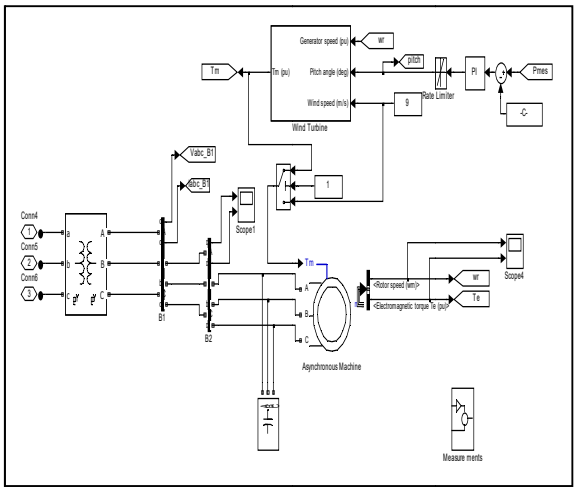

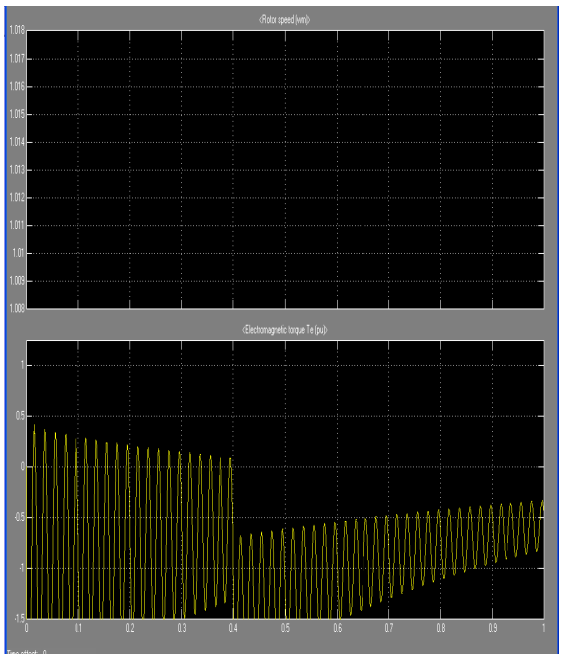

Fig. 4 : Output waveform of wind generator.

II. CONCLUSIONS

Samples like wind,Solar,Hybrid Electrical Vehicles(HEV) and Fuel Cell can be used for making Hybrid model.Hybrid model will utilize both Solar and Wind energy sources.

Wind turbine is designed and is placed with solar panel . This hybrid model will utilize both the sources to generate power.

REFERENCES

[1] Ugur FESLI,Raif BAYIR, "Design and Implementation of a Domestic Solar –Wind Hybrid Energy System"

[2] Peter Van Duijsen,Frank Chen, "Modelling and simulations for Green and Renewable Energy"

[3] First India International Energy Summit-2011

[4] S.D.G.Jayasinghe,D.M.Vilathagamuwa,U.K."Gridsidecascade Inverter system as an Interface for Wind Energy System"

[5] Jinhui xue,Zhongdong Yin,"Technology Research of Novel Energy Storage control for PV Generation"

◈◈◈

Social Welfare Maximization in Deregulated Power System

Rekha Swami

Department of Electrical Engineering, Indian Institute of Technology, Roorkee, India

Abstract - In power systems, transmission network provides the infrastructure to support a competitive electricity market, but congestion occurs frequently in the weakly connected networks. Transmission congestion can enhance the locational market power in the congested area and weaken the efficiency of electricity market. In this paper market dispatch problem in the pool-based electricity market is formulated so as to maximize the social welfare of market participants subject to operational constraints given by real and reactive power balance equations, and security constraints in the form of apparent power flow limits over the congested transmission lines. The comparisons of the real and reactive power costs of generators, benefit value of consumers, producers surplus, locational marginal prices (LMPs) under uncongested or congested conditions are evaluated by using a five-bus system.

Keywords - *Transmission Congestion, market power, locational marginal prices, social welfare.*

I. INTRODUCTION

With the introduction of deregulation in the power industry open access is provided to the transmission system. Due to transmission open access (TOA) the flow in the lines reach the power transfer limit and thereby creating a condition known as congestion [1-3].

The congestion may be caused due to various reasons, such as transmission line outages, generator outages and change in energy demand. Transmission congestion has impact on the entire system as well as on the individual market participants i.e. sellers and buyers. Without congestion lowest-priced resources are used to meet the demand but if congestion is present in the transmission network then it prevents the demand to be met by the lowest-priced resources due to transmission constraints and some energy is purchased from alternative sources at higher prices. The suppliers at the import side may raise their prices as high as they want and thus creates market power, (the conditions where a market participant can profitably maintain prices above a competitive level for a significant period of time) [4-5].

Congestion results an increase in locational marginal prices (LMP), defined as the marginal cost of supplying the next MW of load to the location using the lowest production cost of all available generation without violating any system security limit. If the lowest priced electricity can reach all locations, prices are the same across the entire grid. When there is transmission congestion, energy cannot freely flow to certain locations. In such cases, more expensive electricity is needed to meet that demand and so the locational marginal price is higher in those locations. So its management becomes necessary and this task is performed by Independent System Operator (ISO) [7].

In pool-based electricity market ISO collects hourly/half-hourly supply and demand bids from generator serving traders (GSTs) on behalf of GenCos and load serving traders (LSTs) on behalf of pool consumers. ISO determines the generation and demand schedule as well as LMPs based on maximization of social welfare, subject to system operational and security constraints [8-10].

The supply bids collected by ISO from GenCos are generally for real power generation and reactive power generation is assumed to be produced at negligible cost. In recent developments, the use of reactive power pricing is emphasized in parallel to active power pricing. Many authors have explored the opportunity cost of generators based on P-Q capability curve to develop reactive power generation cost function. Bhattacharya and Bollen *et. Al.* [1] explained the emergence of deregulation from the traditional power industry. Authors of References [2-3] explained the transmission open access in deregulated structure. Li and Bo [6] explained how LMPs are calculated with DC optimal power flow and then comparison is made with AC optimal power flow. Caramanis *et al.* [8] developed the theory of optimal spot pricing, according to which suppliers should be paid real-time price more than or equal to their cost incurred, and consumers should be charged real-time price less than or equal to their benefit, such that overall welfare is obtained. Authors in Ref. [11] discussed technical and economic issues for determining the reactive power pricing structure under an open-access environment. Dai *et al.* [12] modeled the

lost spinning reserve of synchronous generators and depreciation charges on capital investment of capacitor banks to develop a reactive power production cost function. It includes this function into the OPF problem to determine LMPs of real and reactive power. Choi *et al.* [13] performed the maximization of social benefit, representing response (or marginal benefit) of consumers as the inverse of demand function. Singh *et al.* [14] modifies the reactive power generation cost function, as given in [12], by making use of an approximate P-Q capability curve of synchronous generators. The reactive power generation cost function obtained from the P-Q capability curve is added to the real power generation cost function to get total generation cost.

II. PROBLEM FORMULATION

In pool-based electricity market ISO collects hourly/half-hourly supply and demand bids from generator serving traders (GSTs) on behalf of GenCos and load serving traders (LSTs) on behalf of pool consumers. The supply bids provided by a GenCo (or related GST) is its minimum asking price which it would accept for supplying a particular amount of power. Similarly, demand bid of a consumer is its maximum willing price, which it would pay for consuming a particular amount of power. ISO determines the generation and demand schedule as well as locational marginal prices (LMPs) based on maximization of social welfare, subject to system operational and security constraints

The objective function for the optimization problem is to maximize the social welfare, which is the difference of benefit of consumers and the overall cost of active and reactive power production of suppliers. The objective function can be expressed as:

Max. Social Welfare

$$= \sum_{i \in D} B_i(P_{di}) - \sum_{i \in G} C_{pi}(P_{gi}) - \sum_{i \in G} C_{qi}(Q_{gi}) \qquad (1)$$

where {G} is the generator set, {D} is the consumer set, $C_{pi}(P_{gi})$ is the active power production cost of generator i, $C_{qi}(Q_{gi})$ is the reactive power production cost of generator i; $B_i(P_{di})$ is the benefit of the consumer, P_{gi} and Q_{gi} are the active and reactive power output of the generator on bus i, P_{di} is the active power demand on bus i.

The real power generation cost function of each generator is modeled by a quadratic function where a, b and c are predetermined coefficients:

$$C_i(P_{gi}) = a + bP_{gi} + cP_{gi}^2 \ (\$/h) \qquad (2)$$

The reactive power cost of generator is also called as opportunity cost. The reactive power output of a generator will reduce its active power generation capability which can serve at least as spinning reserve, and the corresponding implicit financial loss to generator is modeled as an opportunity cost. For simplicity, the reactive power cost of generator from the approximated capability curve can be modeled as:

$$C_{qi}(Q_{gi}) = [C_i(P_{gi}^{\max}) - C_{qi}(\sqrt{P_{gi}^{\max\,2} - Q_{gi}^2})]k \qquad (3)$$

Where k is the profit rate of active power generation, usually lies between 5 to 10%.

Consumers' benefit as a function of real power demand is considered to follow a straight line passing through origin between $P_{di}^{\min}$ and $P_{di}^{\max}$ which specifies a fixed marginal benefit equal to the slope of line. Using Fig. 1., the benefit of consumer can be written as

$$B_i(P_{di}) = b_{di} * P_{di} \qquad (4)$$

where b_{di} is the slope of benefit curve of consumer at *i*th bus.

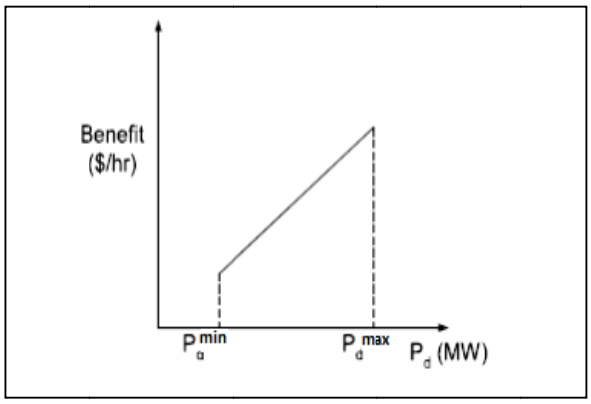

Fig. 1 : Benefit curve of a consumer

CONSTRAINTS

1) Power Flow Equations (Equality Constraints): **A** set of equations that characterizes the flow of real and reactive powers through a system are given by

$$P_{gi} - P_{di} - \sum_{j=1}^{N} V_i V_j Y_{ij} \cos(\delta_i - \delta_j - \theta_{ij}) = 0 \qquad (5)$$

$$Q_{gi} - Q_{di} - \sum_{j=1}^{N} V_i V_j Y_{ij} \sin(\delta_i - \delta_j - \theta_{ij}) = 0 \qquad (6)$$

where N is total number of buses in the system, $\dot{V}_i$ and V_j are the magnitudes of the voltages of bus *i* and *j*, δ_i and δ_j are the voltage angles of bus *i* and *j*, and Y_{ij} and θ_{ij}, are the magnitude and angle of *ij*th element of the bus admittance matrix.

2) Generation Limit: The generators have a maximum generating capacity, above which is not feasible to generate due to technical or economic reasons. Generating limits are usually expressed as maximum or minimum real and reactive power outputs,

$$P_{gi}^{\min} \le P_{gi} \le P_{gi}^{\max} \quad (7)$$

$$Q_{gi}^{\min} \le Q_{gi} \le Q_{gi}^{\max} \quad (8)$$

3) Load Limit: Consumers also have their capacity limits of consumption. Load limits are expressed as follows in the formulation,

$$P_{di}^{\min} \le P_{di} \le P_{di}^{\max} \quad (9)$$

$$Q_{di}^{\min} \le Q_{di} \le Q_{di}^{\max} \quad (10)$$

4) Constraint on constant power factor of loads: The real and reactive power consumption at any bus i are tied together by constant power factor.

$$Qdi = Pdi \tan\alpha i \quad (11)$$

5) Transmission line limits: Transmission limits refer to the maximum power that given transmission line is capable of transmitting under given conditions.

$$S_{ij} \le S_{ij,\max} \quad (12)$$

6) Voltage limits: The voltage at each bus should be within the specified range.

$$V_{i,\min} \le V_i \le V_{i,\max} \quad (13)$$

7) Additional constraint due to capability curve: The apparent power generated by the generator should lie within the boundaries of capability curve.

$$P_{gi}^2 + Q_{gi}^2 \le P_{gi}^{\max 2} \quad (14)$$

The proposed market dispatch problem is a nonlinear programming problem and is solved with Sequential quadratic programming method in AMPL.

III. RESULTS

Five-Bus System:

The methodology described above has been applied on a five-bus system. There are two Gencos at buses 1 and 2, each having lower and upper power generation limits of 10 MW and 200 MW, respectively. The real power generation cost of each Genco is

$$Ci(Pgi) = 75 + 7.5Pgi + .042\,P_{gi}^2 \ (\$/h)$$

The nominal apparent power output of each generator is 125 MVA. The reactive power generation costs of Gencos are modelled using eq. (3), taking k = 5%. In base case, values b_{di} of for all the consumers are set to be fairly high (50 \$/MWh), such that these do not affect generation and demand schedules produced by OPF.

A capacitor bank is installed on bus 4 with total capacity of 50 MVAR can inject capacitive power between 0 to 50 MVAR. The systems loads on buses 1-5 are listed in Table A1 of the Appendix A with a common power factor of 0.9. The transmission line impedance and charging admittance are given in Table A2 of the Appendix A. Lower and upper bus voltage limits are considered to be 0.95 p.u. and 1.05 p.u. Apparent power flow limit of lines is taken to be 180 MVA.

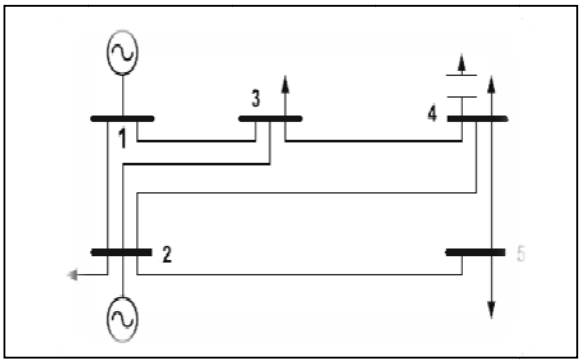

Fig. 2 : Five-bus system

Under heavy loading condition loads on buses 1-5 increase to [0, 0.6, 0.9, 0.8, 1.0] per unit with same power factor of 0.9 and the power generation limits of two Gencos are set to 250 MVA. The system is quite stressed. Now congestion can be created by reducing the flow over line 1-2 by 60 MVA.

Social Welfare Maximization Considering Reactive Power Procurement:

In Table total generation cost, real and reactive power generation costs, power generated values, producers surplus, LMP of real and reactive power at

system buses under congested and un-congested conditions are obtained by the proposed methodology.

As depicted in Table I the benefit values of LSTs become twice with a two fold increase in demand under heavy loading from that of normal loading, because of assumed linear benefit characteristic. But, the social welfare value becomes less than double under heavy loading due to the nonlinear cost characteristics of generators. Although, the reactive power generation cost is small under normal loading, but it increases significantly with increase in loading. This illustrates that there is an utmost need of inclusion of reactive power cost in social welfare maximization.

Table I

Comparison of Results

	Uncongested	**Congested**
Social Welfare ($/h)	6236.90	11045.74
Total Generation Cost ($/h)	2013.1	5454.26
Real Power Generation Cost ($/h)	2012.89	5419.36
Reactive Power Generation Cost ($/h)	0.21	34.90
Benefit Value of Consumer ($/h)	8250.00	16500.00
Power Generation (MW+ j MVAR) $Pg_2 + j\,Qg_2$	82.84 + j 0.73 85.85+ j10.00	118.83+j8.67 223.91+j 109.89
Producers Surplus	447.81	2548.80

The system bus voltage profiles under normal and congested conditions corresponding to proposed results of Table I are shown in Figure 3.

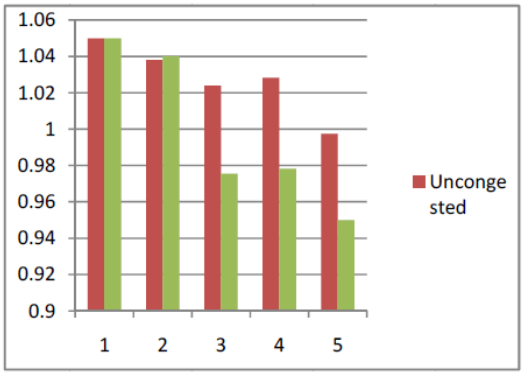

Fig. 3: System Bus Voltage Profile for Uncongested and Congested System

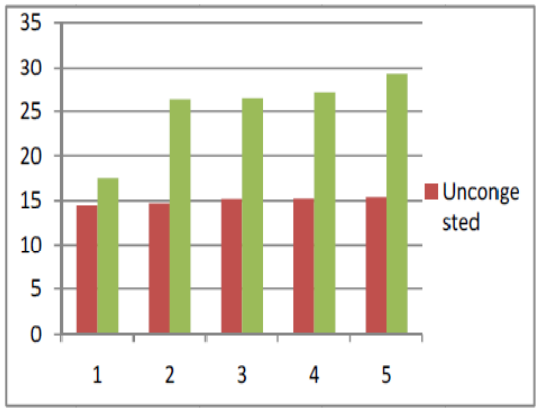

Fig. 4 : LMPs of Real Power for Uncongested and Congested System

From Fig. 4. It can be seen that for uncongested system LMPs for real power and reactive power are low, but when congestion occurs then generators have ability to create market power thereby there will be so LMPs become higher in congested system.

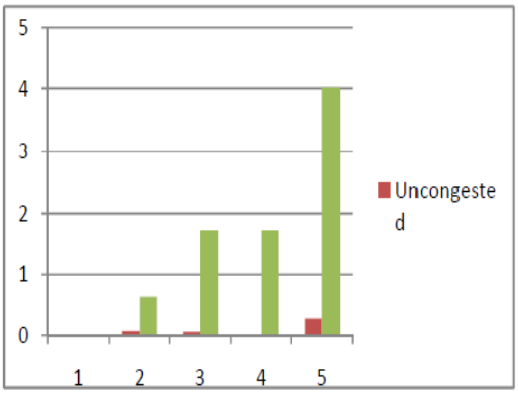

Fig. 5 : LMPs of Reactive Power for Uncongested and Congested System

IV. CONCLUSION

In this paper, market dispatch problem with the objective of maximization of social welfare is solved in the pool-based electricity market. From the optimization results given of five-bus system it can be concluded that although the presence of congestion results in an increase in market power along with producer surplus but with the given methodology there is also increase in consumers benefit value. So with the proposed method each market participant i.e. sellers or buyers are getting benefit in the case of congestion in the electricity market.

Appendix A

Table A1 Test system loads

Bus	Active Power	Reactive Power
1	0.0	0.0
2	0.20	0.097
3	0.45	0.22
4	0.40	0.19
5	0.60	0.29

Table A2 Test system line data

Bus node	Line impedance z_{ij}	Line charging y_{ij}
1-2	0.02 + j0.06	0.0 + j0.030
1-3	0.08 + j0.24	0.0 + j0.025
2-3	0.06 + j0.18	0.0 + j0.020
2-4	0.06 + j0.18	0.0 + j0.020
2-5	0.04 + j0.12	0.0 + j0.015
3-4	0.01 + j0.03	0.0 + j0.010
4-5	0.08 + j0.24	0.0 + j0.025

REFERENCES

[1] Kakar Bhattacharya, Math H.J. Bollen and Jaap E. Daalder, Operation of Restructured Power Systems, Chalmers University of Technology, Kluwer Academic publishers, 2001.

[2] Mohammad Shahidehpour, Hatim Yamin and Zuyi Li, Market Operations in Electric Power Systems, Published by John Wiley & Sons Ltd, 2002.

[3] Loa Lei Lai, Power System Restructuring and Deregulation, Published by John Wiley & Sons Ltd, 2002.

[4] A. Kumar David and Fushuan Wen, Market Power in Electricity Supply, IEEE Transactions on energy conversion, Vol. 16, No. 4, pp. 352-360, December 2001.

[5] R. Moreira e Silva and L.D.B. Terra, " Market power under transmission congestion constraints,'' in Proc. 1999 International Conference on Electrical Power Engineering, pp. 82.

[6] Fangxing Li, Rui Bo, DCOPF-Based LMP Simulation: Algorithm, Comparison With ACOPF, and Sensitivity, IEEE Trans. Power Syst., Vol. 22, No. 4, pp. 1475-1485, November 2007.

[7] S. Charles Raja, P. Venkatesh, B.V. Manikandan, Transmission Congestion Management in Restructured Power Systems, Proc. of ICETECT 2011.

[8] Caramanis, M. C., Bohn, R. E., and Schweppe, F. C., "Optimal spot pricing: Practice and theory," IEEE Trans. Power Apparatus Syst., Vol. PAS-101, pp. 3234–3245, September 1982.

[9] Baughman, M. L., and Siddiqi, S. N., "Real-time pricing of reactive power: Theory and case study results," IEEE Trans. Power Syst., Vol. 6, pp. 23–29, February 1991.

[10] Gedra, T. W., On transmission congestion and pricing, IEEE Trans. Power Syst., Vol. 14, pp. 241–248, February 1999.

[11] Hao, S., and Papalexopoulos, A., "Reactive power pricing and management," IEEE Trans. Power Syst., Vol. 12, pp. 95–104, February 1997.

[12] Dai, Y., Ni, Y. X., Shen, C. M., Wen, F. S., Han, Z. X., and Wu, F. F., "A study of reactive power marginal price in electricity market," Elect. Power Syst. Res., Vol. 57, pp. 41–48, 2001.

[13] J.Y. Choi, S. Rim, J. Park, Optimal real time pricing of real and reactive powers, IEEE Trans. Power Syst., Vol. 13, No. 4, pp. 1226–1231, 1998.

[14] Kanwardeep Singh, N. P. Padhy , J. D. Sharma, Social Welfare Maximization Considering Reactive Power and Congestion Management in the Deregulated Environment, Electric Power Components and Systems, pp. 50-71, Dec. 2009.

◈◈◈

The Factors Affecting Energy Management System Adoption for Smart Home : Marketing Survey Approach

Jyh-Yih Hsu & Jung-Jui Chang

Department of Management Information Systems, National Chung Hsing University, Taichung, Taiwan

Abstract - This paper explores the factors that affect households' adoption for Home Energy Management System. A market survey is conducted and Chi-square test is applied as research methodology. The research results reveal that households' general knowledge of energy saving and carbon reduction, daily behaviors, and cognitive have a significant correlation to households' intention to adopt Home Energy Management System. Finally, we infer possible explanations according to our results.

Keywords - *Energy Management System, Smart Home, AMI, Marketing Survey.*

I. INTRODUCTION

Nowadays, Advanced Metering Infrastructure (AMI) and Energy Management have been the topic of intense research. AMI refers to the full measurement and collection system, including smart meters, communication networks, and data management systems [1]. AMI with smart meters, In-Home Displays, and Programmable Communicating Thermostats enables households to assist in using energy more efficiently and adjust their behavior to reduce peak capacity required [2].

Because of the development of AMI, electricity consumption information has become more transparent to households. To make a fully display of home appliances electricity consumption, we need to establish Energy Management System, including smart meters , In-Home Displays, and energy management database to record and feedback electricity consumption information or receive control commands [3]. Many companies and institutes all over the world are doing the research and developing on Energy Management System, with tremendous results have been achieved [4], which in the field of demand response, time of use, and electric vehicles.

In Taiwan, Home Energy Management System has not been widely adopted in the community. Accordingly, the objectives of this study are understanding the current of households' attributes of Home Energy Management System and finding the correlation between households' general knowledge of energy saving and carbon reduction, life behaviors and cognitive and willingness for adopting Home Energy Management System. In order to achieve these goals, this study conducts a market survey and uses Chi-square test to identify the collected data.

The rest of this paper is organized as follows. In Section II, we describe AMI and Home Energy Management System. Methodology of this paper utilized is shown in Section III. Research results are presented in Section IV Finally, we conclude with some contributions of this paper in Section V.

II. LITERATURE REVIEW

A. Advanced Metering Infrastructure

AMI has composed of Smart Meter, Communication System and Meter Database Management System. It provides two-way communication to the electric meter to enable time stamping of meter data, outage reporting, communication into the customer premise, service connect/disconnect, on-request reads, and other functions [5].

AMI can support Power Company doing automatic meter reading, instead of wasting time and manpower for manual meter reading operations in the past. In addition, it provides those power companies with opportunity for the improvement of checking outage and devising how to deal with the outage [6]. Generally, it not only reduces the labor cost and increases meter-reading accuracy but also provides accurate load information and billing data to help customers manage their power consumption [7].

In Taiwan Power Company's (TPC) AMI programming, they focus on formulating AMI standard, building open testing platform, and providing enterprises testing meters, communication network,

Meter Database Management System, Information security and availability. TPC has begun developing high-voltage AMI in 2009, and completed 23,000 high-voltage users' smart meter installation in 2012. About low-voltage, according to international trends and Taiwan industry overviews, Ministry of Economic Affairs has developing AMI program, including four stages, that is Technical testing, Pre-developing, Basic developing, and Expanded developing. Table I shows the details of developing schedule in Taiwan.

Xxxx

Table I. Taiwan Power Company's AMI developing schedule

	First stage (Tech. test)		Second stage (Preliminary Installation)			Third stage (Fundamental Installation)				Fourth stage (Extended Installation)
Year	2009	2010	2011	2012		2013	2014	2015		After 2016
Meter No.	50	300-500	10,000		Technology Confirm & C/B Ass.	1,000,000			Cost/Benefit Assessment	5,000,000
Working Items	• Communication Technology Testing	• Define Function and Standard • Test Platform Plan	• MDMS Meter Function Test • Meter Function Std. ID. • Construct Test Platform • Construct New TOU Fee			• Meters Installation • New TOU Fee Execution • Load Management and Demand Response Study				• Construct Distribution Automation System • Apply Load Management and Demand Response

Source: Taiwan Power Company

Xxxx

B. Home Energy Management System

Energy management can be divided into the macro-level management and micro-level management. In the macro-level management, it mainly refers to the formulation of policies and regulations; in the micro-level management, it mainly through the day-to-day operation to achieve energy saving [8].

There are four main points of energy management, first is reducing overall electricity demand; second is converting peak time demand to off-peak time; third is increasing electricity demand in off-peak time; finally is decreasing electricity demand in peak time. For enterprises, energy management can improve enterprises' competitiveness [9]; for households, through the transparency of electricity information, households can clearly understand current electricity price, electricity price is higher during peak hour and lower during off-peak hours. Households can adjust power consumption along with timing [3].

Home Energy Management System is integrating with many technologies, such as electric measurement,

monitor system, human-computer interface, and network communication [10]. It can record and analyze electric data, schedule electrical load, and collect meter information through internet [11]. It provides updated energy and budgeting information to give users help of optimizing home energy use. Users can gain visibility into household energy usage and control how energy is utilized with the Energy Management System [3].

Few literatures discuss the factors that affect consumer to adopt Home Energy Management, so that the paper focuses on this topic and investigates the factors.

III. METHODOLOGY

Home Energy Management System has not been widely adopted in the community. Why is that? This research attempts to find the reason and identify the factors that affect the customers' willingness to adopt Home Energy Management System.

Consumer behavior is the study of individuals, groups, or organizations and the processes they use to select, secure, use, and dispose of products, services, experiences, or ideas to satisfy needs and the impacts that these processes have on the consumer and society (Kotler, 1997). The main factors that influence consumer making decisions can be divided into the

following three categories: (1) environmental impacting factors, including cultures, family, social stratum, and situations; (2) personal difference factors, including knowledge, attitude, incentives and involvement, consumer's source, personality value, and lifestyle; (3) psychological factors, including learning, attitude, behavior changing, and information handling (Engel and Fetal, 1973).

Questionnaire Survey method is adopted in this paper. The research process is following six steps: (1) Background information and literatures review; (2) Discuss and design the questionnaire; (3) Pre-testing; (4) Revise the questionnaire; (5) Internet survey the completed questionnaire; (6) Retrieve the questionnaire and analyze the results.

Then, we upload our questionnaire on the platform of "mySurvey" at www.mysurvey.tw. During the period from December 10 2011 to July 31 2011, the total number of retrieving the questionnaire sample is 123. According to the demographic information of respondents in Table II, there are 76 male and 47 female. In these 123 respondents, there are 59 reluctant to use Home Energy Management System, and 64 are willing to adopt the system. In these 59, nearly 60% think the price of Home Energy Management System is too expensive, and 24% consider the actual effectiveness of Home Energy Management System may not be as expected. (See Table III)

Table II. Demographic information of respondents

Demographic profile		Numbers	Percentage
Gender	male	76	61.79%
	female	47	38.21%
Age	< 20	4	3.25%
	20-29	67	54.47%
	30-39	22	17.89%
	40-49	14	13.01%
	> 50	16	11.38%
Education	Under or junior high school	0	0%
	senior high school	19	15.45%
	University	57	46.34%
	Graduate school or above	47	38.21%
Total		123	100%

Table III. The reasons of people reluctant to use the Home Energy Management System

Question	Options	Numbers	Percentage
Why you don't use Energy Management System?	Too expensive	35	59%
	The actual effectiveness may not be as expected	14	24%
	Don't understand the real usefulness	8	13%
	Ineffective to save electricity	1	2%
	Busy to work, don't have time to consider this matter	1	2%
Total		59	100%

IV. RESEARCH RESULTS

We use Chi-square test to identify the correlation; the X_0^2 can be calculated by the following formula:

$$X_0^2 = \sum_{i=1}^{c} \sum_{j=1}^{r} \frac{(o_{ij} - e_{ij})^2}{e_{ij}} \qquad (1)$$

Definitions:

c is the number of columns

r is the number of rows

o_{ij} is the real observed values

e_{ij} is the expected values

1) Test the correlation between "are you willing to adopt home energy management system" and "aware of the government has implemented energy saving policies". We make the following hypothesis:

H_0: There is a correlation between "are you willing to adopt home energy management system" and "aware of the government has implemented energy saving policies".

H_1: There isn't a correlation between "are you willing to adopt home energy management system" and "aware of the government has implemented energy saving policies".

Table IV. The survey results of respondents' knowledge

	Willing	Not willing	Total
Aware of	39	24	63
Not aware of	25	35	60
Total	64	59	

Through Chi-square test, α is 0.05, we get the X_0^2 is 4.03 and $X_{0.95}^2$ is 3.84. The result accepts H_0 ($X_0^2 > X_{0.95}^2$); in other words, it shows that there is a correlation between "are you willing to adopt home energy management system" and "aware of the government has implemented energy saving policies". It represents households who know the government has implemented energy saving policies are more willing to adopt Home Energy Management System.

2) Test the correlation between "are you willing to adopt home energy management system" and "do you concern the information of energy conservation". We make the following hypothesis:

H_0: There is a correlation between "are you willing to adopt home energy management system" and "do you concern the information of energy conservation".

H_1: There isn't a correlation between "are you willing to adopt home energy management system" and "do you concern the information of energy conservation"

Table V. The survey results of respondents' cognition

	willing	not willing	total
concern*	54	35	89
no concern**	10	24	34
total	64	59	

* "concern" means "concern the information of energy conservation"

** "no concern" means "don't concern the information of energy conservation"

Through Chi-square test, α is 0.05, we get the X_0^2 is 31.28 and $X_{0.95}^2$ is 3.84. The result accepts H_0 ($X_0^2 > X_{0.95}^2$); in other words, it means that there is a correlation between "are you willing to adopt home energy management system" and "do you concern the information of energy conservation". It represents households who have more concerned about the information of energy conservation are more willing to adopt Home Energy Management System.

3) Test the correlation between "are you willing to adopt home energy management system" and "households' knowing electricity payment per month". We make the following hypothesis:

H_0: There is a correlation between "are you willing to adopt home energy management system" and "households' knowing electricity payment per month".

H_1: There isn't a correlation between "are you willing to adopt home energy management system" and "households' knowing electricity payment per month"

Table VI. The survey results of respondents' daily behavior

	Willing	Not willing	Total
Below 500 dollars	10	13	23
Between 501 and 1000 dollars	17	20	37
Between 1001 and 1500 dollars	19	13	32
Between 1501 and 2000 dollars	6	4	10
Above 2001 dollars	8	6	14
Don't clear	4	3	7
total	64	59	

Through Chi-square test, α is 0.05, we get the X_0^2 is 37.95 and $X_{0.95}^2$ is 11.07. The result accepts H_0 ($X_0^2 > X_{0.95}^2$); in other words, it means that there has correlation between "are you willing to adopt home energy management system" and "households' knowing electricity payment per month". It represents households who have more electricity costs per month are more willing to adopt Home Energy Management System.

V. CONCLUSIONS

This paper investigates the correlation between households' general knowledge of energy saving and carbon reduction, life behaviors and cognitive and willingness of adopting Home Energy Management System. According to the research results, we find that there is a positive correlation. It represents households who have those traits are more willing to adopt Home Energy Management System. Therefore, we infer that maybe we can enhance households' knowledge of energy saving and carbon reduction, encourage households to save energy from daily behaviors. According to our analysis results, these applicable methods will enhance the willingness to adopt Smart Home Energy Management System.

In this study, there are some limitations. Firstly, most of respondents are youngsters, so that the research result has a bias in findings which maybe not applicable to people in other ages. Secondly, most of respondents are students and average income is under 25,000 per month, so that the research result does not cover the households with high income and not comprehensively

represent all ranks of different income level deeply. For directions future research, researchers can do the research of finding the difference between the households with high income and general households, and how the willingness of adopting Home Energy Management System.

REFERENCES

[1] Crossley, "Smart Metering, Load Control and Energy-using Behaviour," Workshop on Smart Metering to Use Less Energy, Brugge, Belgium, 2007.

[2] Jun Wang and C. M. Leung, "A Survey of Technical Requirements and Consumer Application Standards for IP-based Smart Grid AMI Network," Proc. International Conf. on Information Networking (ICOIN 11), Barcelona, Jan. 2011 pp. 114-119, doi:10.1109/ ICOIN.2011.5723144.

[3] C. W. Liu, C. C. Luo, P. Y. Lin, G. C. Lu, W. C. Wu, J. I. Tsai, C. Y. Hsueh, "Develop a power quality measurement system integrated with HAN home energy management system," Proc. International Conf. on Electric Utility Deregulation and Restructuring and Power Technologies (DRPT 11), Shandong, Jul. 2011 pp. 1506-1510, doi:10.1109/ DRPT.2011.5994135.

[4] N. Jinrui, S. Fengchun, and R. Qinglian, "A Study of Energy Management System of Electric Vehicles," Proc. Vehicle Power and Propulsion Conference (VPPC 06), Windsor, United Kingdom, Sep. 2006, pp. 1-6, doi:10.1109/VPPC.2006.364301.

[5] D. G. Hart, "Using AMI to Realize the Smart Grid," Power and Energy Society General Meeting Conversion and Delivery of Electrical Energy-Conversion and Delivery of Electrical Energy in the 21st Century, IEEE, pp. 1-2, 2009.

[6] S. H. Choi, S. J. Kang, N. J. Jung, and I. K. Yang, "The design of outage management system utilizing meter information based on AMI (Advanced Metering Infrastructure) system," Proc. International Conf. Power Electronics and ECCE Asia (ICPE & ECCE 11), IEEE, Jeju, Korea, Jun. 2011 pp. 2955-2961, doi:10.1109/ICPE.2011.5944797.

[7] H. Sui, H. Wang, M. S. Lu, and W. J. Lee, "An AMI System for the Deregulated Electricity Markets," Proc. IEEE Trans. Industry Applications, IEEE press, Dec. 2009, vol. 45, no. 6, pp. 2104-2108, doi:10.1109/ TIA.2009.2031848.

[8] Y. Wu, "Scientific Management-the First Step of Building Energy Efficiency," Proc. International Conf. on Information Management, Innovation Management and Industrial Engineering, Xi'an, China, Dec. 2009, vol. 4, pp. 619-622, doi:10.1109/ICIII.2009.608.

[9] A. B. Kipnis "Audit cultures: Neoliberal governmentality, socialist legacy, or technologies of governing?" American Ethnologist, vol. 35, May 2008, pp. 275–289, doi:10.1111/j.1548-1425.2008.00034.x.

[10] C. S. Choi, W. K. Park, J. S. Han, and I. W. Lee, "The Architecture and Implementation of Proactive Green Home Energy Management System," Proc. International Conf. on Information and Communication Technology Convergence (ICTC 10), Hangchow, Nov. 2010, pp.457-458, doi:10.1109/ICTC.2010.5674798.

[11] H. Joe, J. Park, C. Lim, D. Woo, and H. Kim, "Instruction-Level Power Estimator for Sensor Networks," ETRI Journal, vol.30, Feb. 2008, pp.47-58, doi:10.4218/etrij.08.0106.0240.

◈◈◈